ISSN No:-2456-2165

Application of the Unified Scale to the Characterization of Seismic Activity of the Democratic Republic of Congo and its Surroundings

(Comparative study for Africa, Indonesia and the Pacific coast of Central America)

Anscaire MUKANGE BESA[1], ZANA NDOTONI[1,2].
[1]Department of Physics, Faculty of Sciences, University of Kinshasa, Kinshasa, DR Congo.
[2]Department of Internal Geophysics, Center of Research in Geophysics (CRG), Kinshasa, DR Congo.

Abstract:- The design of the unified scale for characterizing the seismic activity of an area requires its testing. Thus, we applied this model to the characterization of the seismicity of the Democratic Republic of Congo (DRC: 10°E-35°E; 14°S-6°N). For a better evaluation, this model has been extended to other areas, including the African Continent (15°W-60°E: 25°S-55°N) -, Indonesia (125°E-150°E ; 10°S-10°N) and the Pacific coast of Central America (115°W-90°W; 0°N-20°N) for the period from 1975 to 2013.

The application of the unified scale to characterize the seismicity of these areas has provided satisfactory results. Indeed, the identification of the seismic species in each Zone-Grid (mesh) and the attribution of the seismic level (modulus) and the corresponding color code, the use of the similarity rate parameter as well as the introduction of the representation of an area as a vector, allowed:

- **The development of a device (clock) called Acti-seismometer to better follow the seismic activity and the geodynamics of an area**
- **Modeling of the internal structures of an area using equations, curves (signatures), zoning maps (tomography) ...**
- **Demonstration of the clear difference between the seismicity of the rift zones (25-35°E), marked by high activity and that outside the rift (10-25°E), of low activity;**
- **The identification of a transition zone between the aforementioned zones, located between (20-25°E),**
- **The identification of earthquake zones located in the sedimentary zone (Congolese craton) where geophysical research has revealed the presence of hydrocarbons,**
- **The seismic risk assessment in each Grid Zone of the DRC which; unlike the classic model, ours indicates a high seismic risk at:**
  - **Zone A23 (Kinshasa-Bandundu and surroundings), following, in particular, the presence of the Kinshasa nuclear power plant, and the presence of faults observed in its surroundings, not to mention the high density of the population,**
  - **Zone A42 (Kivu): the risk is significant there following the presence of volcanoes (Nyiragongo, Nyamulagira, etc.) whose flow is heading towards the city, presence of Lake Kivu containing harmful gas (methane gas and dioxide of carbon) and the presence of complex faults observed there, not to mention the high density of the population,**
- **The comparison of the structures of the Africa, DRC, Indonesia and Pacific Coast zones of Central America where we observe that the hypocentres go in increasing order DRC-Pacific Coast - Indonesia.**

Our characterization model will make it possible to map various parts of the globe and compare them with each other with the possibility of exploiting it for geological prospecting: For a better assessment of the seismic risk, the area of the study area should be reduced.

Keywords:- *Unified Scale, Characterization, Modulus, Seismic Risk, Internal Structure, Signature, Resemblance Rate, Acti-Seismometer, DRC*

I. INTRODUCTION

Having designed the unified characterization scale, we now want to test it for the characterization of the seismicity of the Democratic Republic of Congo (DRC). For better control, we are extending our research to other areas such as the African continent, Indonesia and the Pacific coast of Central America (Fig.1.2). For the DRC, the study goes as far as seismic risk assessment in its various areas.

The East African Rifts system is presented as a continental extension of the world system of lithospheric fractures which meander through the middle of the Atlantic and Indian Oceans and which extend into the eastern part of the African Continent via the Gulf of Aden and the Red Sea (Mukange, 2016 ; Boden et al. 1988 ; Bantidi, 2014a)This fracture system consists of two branches, namely :

- **The Eastern Branch** which, from the Afar triangle, crosses Ethiopia and Kenya to the northern Tanzanian divergence (Fig. (1.1);Mukange, 2013).
- **The Western Branch** is made up of a system of fractures which cross the Great Lakes garland, that is to say, from Lake Albert passes through lakes Edward, Kivu, Tanganyika, Rukwa, Malawi and continues south to Mount Beira in Mozambique and southwest of Lake

ISSN No:-2456-2165

Kariba, Zimbabwe (Fig.1.1). This branch therefore covers most of the eastern provinces of the DRC from latitude 4 ° N to latitude 8 ° S. However, the seismic activity of the DRC also includes that characteristic of intraplate fractures which thus affects the entire Congolese basin known as the "Congolese craton" (Fig.1.2).

The seismic activity recorded here and there and the extent of the zones it affects reveal the need for its characterization with a view to assessing the seismic risk potential. This assessment must be constantly and regularly updated with new data and translated into a seismic zoning map(Mukange, 2013).

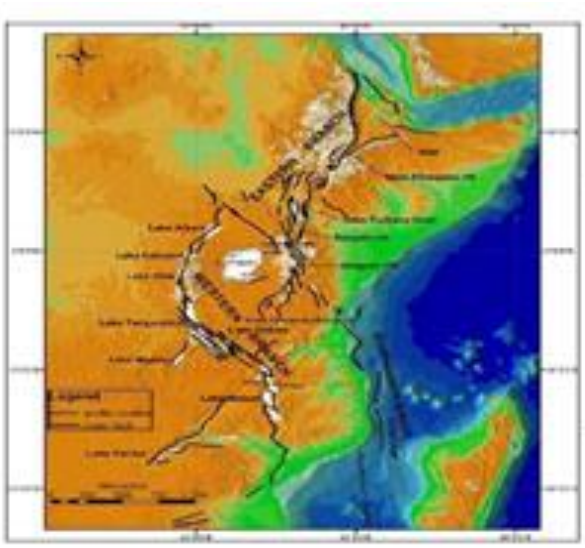

Fig.1.1: The East African rift system [2]

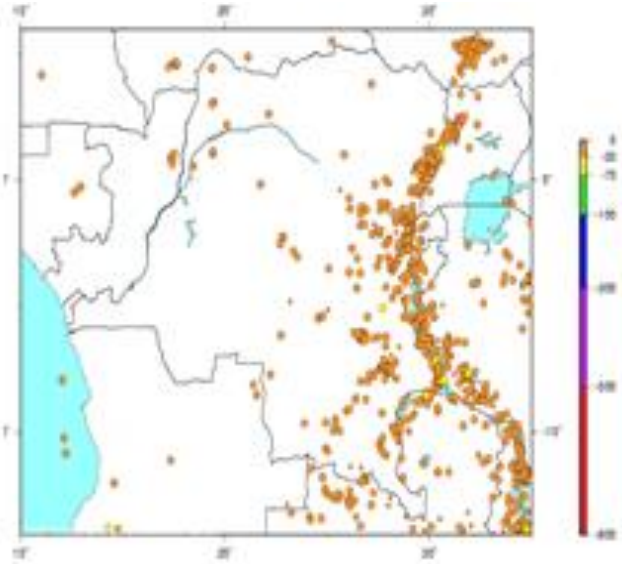

Fig. 1.2: Distribution of epicenters of the DRC (1973-2008).

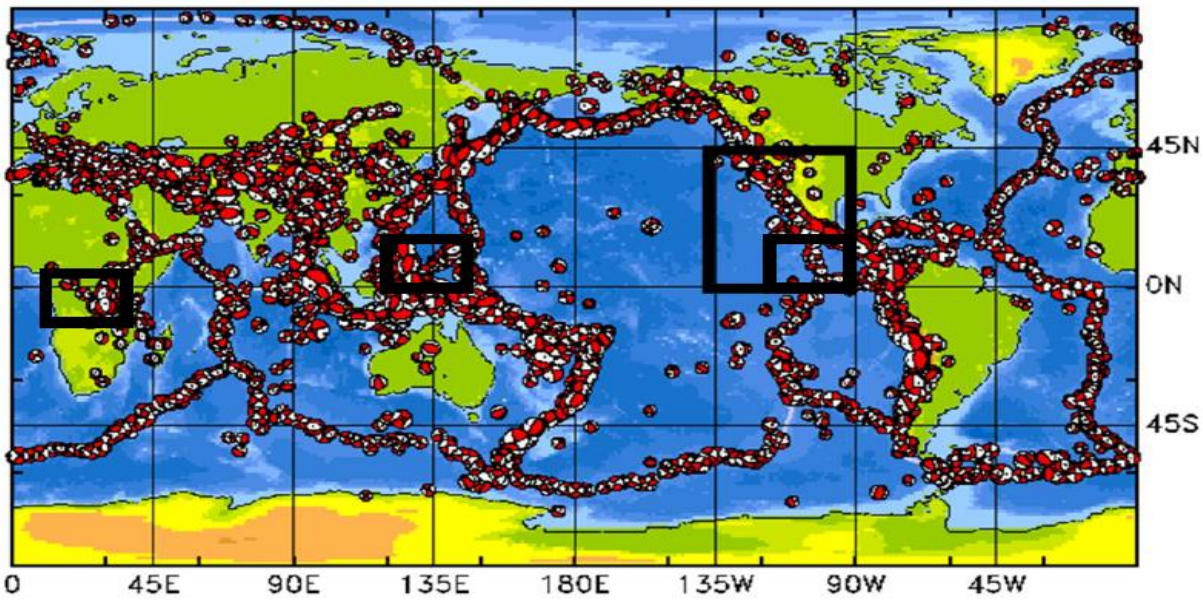

Fig. 1.3.: Location of the Study Areas (rectangle in black)

II. DATA AND METHOD OF ANALYSIS

2.1. Analysis data

To do this, we analyze the data collected through various sources (www.usgs.org and www.isc.ac.uk), but reunited in a single scale, covering the period from 1910 to 2013 over the geographical area included between 6°North and 14°South latitude and between 10°East and 40°East longitude. This geographical area includes entirely the DRC, Rwanda, Burundi and partially the neighboring countries, such as Uganda, Zambia, South Sudan, Tanzania, Gabon, Angola, Cameroon and Congo-Brazzaville (Fig.1.2).

The characteristics of the DRC's seismicity are deduced from the analysis of the classical parameters evaluated for each zone and sub-zone (Mukange, 2021).

ISSN No:-2456-2165

2.2 Method of analysis

The method used consists of subdividing the territory of the DRC into sub-zones based on the approach with or without a seismic source. Thus, we have the so-called zone-provinces, at the limits close to those of the former provinces of the DRC and the zones called rift zones because they are located in the western branch of the Rift-Valleys (Fig.2.1).

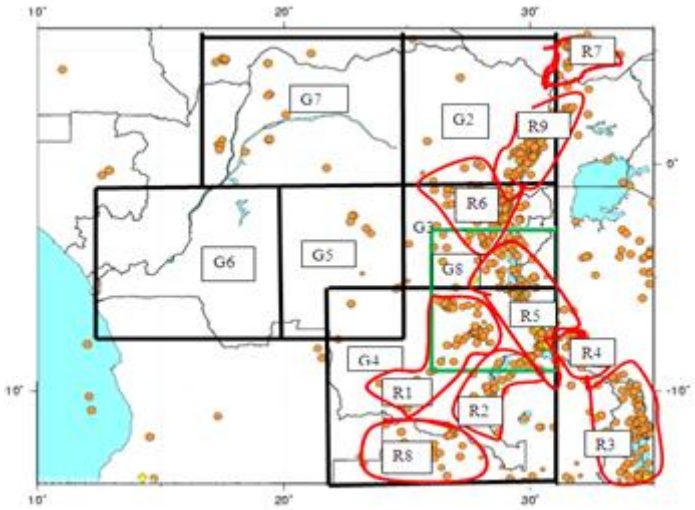

Fig.2.1: Limits of provincail regions in black rectangle (Gi) and limits of Rift regions in red or green (Rn), (Mukange, 2011).

The development of a device (clock) called Acti-seismometer allowing the best possible follow-up of the seismic activity and the geodynamics of an area through the control of parameters, including the variation of the area, of the perimeter, rotation speed,…. ,… .This was only made possible thanks to the introduction of the concept of circular or polar representation of the seismic activity of zones.

The seismic level being dynamic, makes it possible to describe the seismic activity (and the geodynamics) of an area over time, hence a better monitoring of the seismic activity, hence the invention of a device called acti-seismometer , The generation of a "seismic species" linked to the seismic activity of each of the zones unambiguously associates a corresponding quantified seismic level, a device called an acti-seismometer.

However, we are particularly interested in dividing the territory into meshes, also called Grid Zones (Mukange, 2021b).

This approach consists of subdividing the territory under study into subzones or vertical (columns) and horizontal (rows) bands in steps of five degrees. The intersections of these bands form meshes, called Zone-Grids (Tables (2.1-2); Fig (.3.4) and Fig. (3.9)). As a reminder, for quick calculations, we take 1° equals 111.111km (André, 1980).

Table 2.1: Division of the territory of the DRC into vertical zones: West-East

N°	Area	Area boundaries (columns)		Number of earthquakes
		Longitude	Latitude	
1.	A1	10°E-15°E	14°E-6°N	23
2.	A2	15°E-20°E	14°S-6°N	40
3.	A3	20°E-25°E	14°E-6°N	232
4.	A4	25°E-31,3°E	14°S-6°N	1905
5.	A5	31,3°E-35°E	14°E-6°N	1345

Table 2.2: Division of the territory into horizontal zones: from North to South

N°	Area	Area boundaries (Lines)		Number of earthquakes
		Longitude	Latitude	
1.	B1	10°E-35°E	6°N-1°N	365
2.	B2	10°E-35°E	1°N-4°S	1338
3.	B3	10°E-35°E	4°S-9°S	1087
4.	B4	10°E-35°E	9°S-14°S	736

ISSN No:-2456-2165

III. PRESENTATION AND DISCUSSION OF THE RESULTS

3.1. Presentation of the results

Below we present the results of our work. $\log N = a - b\, m_b$

3.1.1. Earthquake statistics: b-value, λb-value and intercepts

Statistics on the frequency of earthquakes in a region have long been characterized by the number (N) of earthquakes felt or recorded on average per year or for a defined period. If N is the annual number of earthquakes of magnitude between (m-0.5 and m + 0.5) for example, the following linear decrease has been established (Lay and al. 1995):

$$\log N = a - bm_b \qquad (3.1)$$

Where, the constants a and b are obtained by applying the law of least squares.

The constant b is called "value b" (b value in English), generally between 0.5 and 1. But it can sometimes reach the value 2.5 for the swarms of the earthquakes. The ratio of "a" to "b" gives the calculated maximum magnitude that can be recorded in the area concerned; for the territory of the DRC, we have mbmax = 7.4 whereas that observed is 7.5 in Lake Tanganyika, in 1910 (Fig. 3.1).

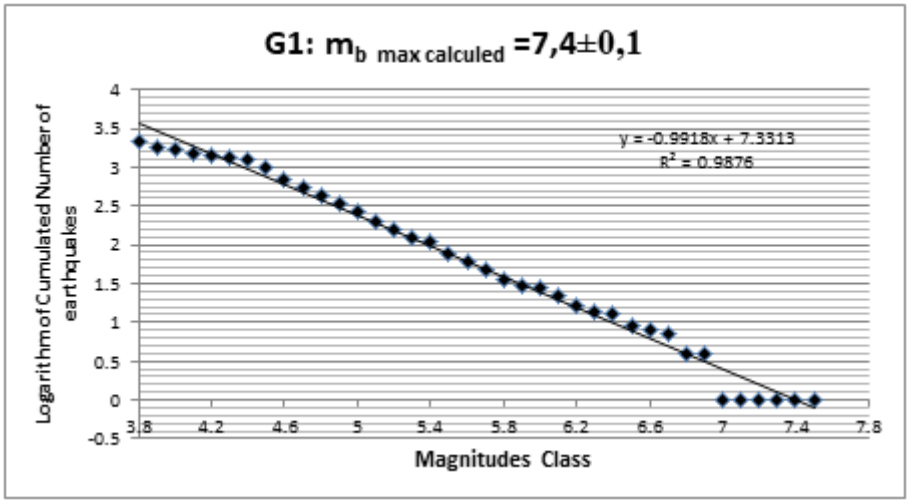

Fig. 3.1. : Earthquake statistics of the DRC (G1) deduced from relation (1.5)

For better comparison, we prefer to convert the cumulative number of earthquakes per magnitude range as a percentage of the total number of earthquakes recorded in an area; the exponential curve of figure (3.2) obtained from (mb-% Number of earthquakes) leads to a constant, called λb-value that we can relate to the b-value. Likewise, if we draw the trendline by least squares, we obtain a straight line which intersects the abscissa axis at a point, called the intercept Ix which we can also relate to the maximum calculated magnitude obtained from the b-value.

In our case, $\lambda_b = 2.28$ and $I_x = 137.1/20.99 = 6.532$ **(3.2)**

Starting from Figure (3.2), we define the parameters λb-value and the intercept Ix as expressed by relations (3.3) and (3.5):

$$Y = N_0 \exp(-\lambda_b x) \qquad (3.3)$$

In the framework of figure (2.16), $\lambda_b = 2,28$ **(3.4)**

and

$$Y = ax + b \text{ et } I_x = -b/a \qquad (3.5)$$

ISSN No:-2456-2165

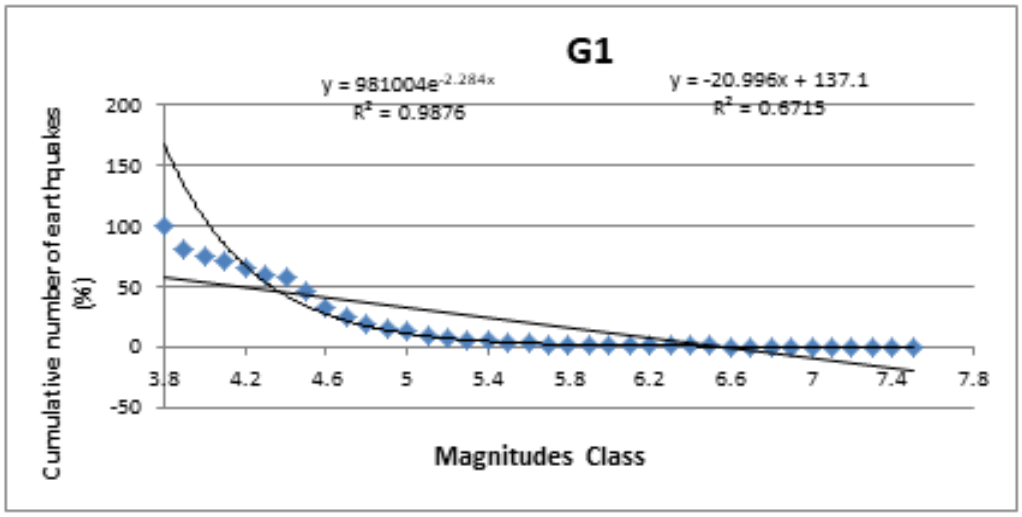

Fig.3.2: Earthquake statistics in the DRC, deduction of the parameters λb-value and the intercept.

The following relation relates $\lambda_{b\text{-value}}$ to b-value.

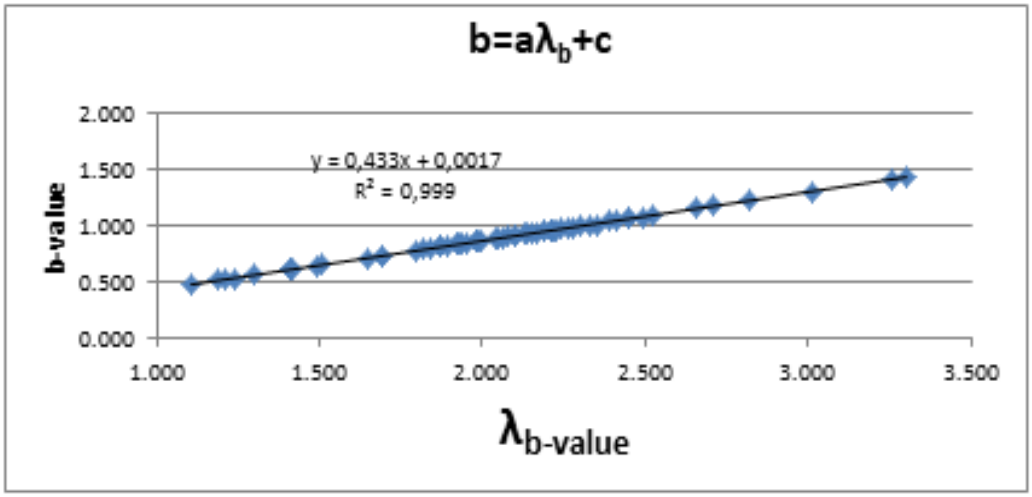

Fig. 3.3: Linear relation between the λb-value and the b-value for the whole DRC (G1)

In DRC, b-value is related to $\lambda_{b\text{-value}}$ by the relation:

$$b = 0.433\,\lambda_b + 0.001 \qquad \textbf{(3.6a)}$$

The study we have just extended to other areas of the globe, notably the Pacific-North side of the American continent and Indonesia, shows that this relationship is almost identical and therefore universal; she wants :

$$\lambda_{b\text{-value}} \approx 2{,}304\,b \qquad \textbf{(3.6b)}$$

This would therefore be a new parameter that has just emerged in seismology.

3.1.2. Assignment of the seismic species and level corresponding to a few zones

The processing of the data and the application of the model give the results contained in table (3.1.) Below, in particular in the last column which presents the seismic species and its level of activity (figure).

3.1.3. Assignment of the seismic level (modulus) to each Zone-grid (mesh)

Our work has mainly focused on the subdivision of the territory of the DRC and others into grid or mesh zones. The territory is therefore subdivided into four lines (L1, L2, L3, L4) and five columns (C1, C2, C3, C4, C5) whose intersections form the mesh Aij (Figure below).

Table 3.3. : Seismic parameters calculated and observed for the DRC Zones-Provinces: seismic species and characterization scale

AREAS	LIMITS OF AREAS STUDIED	MAXIMUM MAGNITUDE ACHIEVED (m_{bo}) AND CALCULED (m_{bc}),INTERCEPTED (I_x), Area(A)					ENERGY (E_T), NUMBER(N_T) DES EARTHQUAKES RELEASED		SEISMIC ACTIVITY(%), FREQUENCY(f), DENSITY(D)		CLASS (MAGNITUDE)								LADDER AND SEISMIC SPACE
											I: $4 \leq m_{bo} \leq 4,9$		II: $5 \leq m_{bo} \leq 5,9$		III: $6 \leq m_{bo} \leq 6,9$		IV : $7 \leq m_{bo} \leq 8$		
	Longitude	$m_{bobservée}$	m_{bc1}	Log Mo	A	I_x	N_T	E_T	Ann.	f	N	T(an)	N	T	N	T	N	T	Level zoning in Arabic numerals
	Latitude	Log Moc	b	c	λ_b		Rate (%)	Rate (%)	Moth.	D	Rate (%)		Rate (%)		Rate (%)		Rate (%)		
G2 P.EASTEN	25°E-31,3°E	6,9	6,8	26,3	42	6,153	594	312 E+20	98%	9,9	514	0,12	72	0,83	5	20,8	0	-	IIIababbb
	0,7°S-6°N	26,22	0,981	1,31	2,26		17 %	3,4%		0,24	**87**		**12**		**1**	**1,31**	0		25
G3 P .KIVU	25°E-31,3°E	6,5	6,8	25,8	27	6,00	678	130 E+20	98%	11,3	600	0,1	70	0,86	7	14,9	0	-	IIIaaabbbb 14
	0,7°S-6°N	26,482	1,023	0,86	2,35		19 %	1,4%		0,42	**88,6**	**27**	**10,3**		**1**	**1,34**	0	-	
G4 P.KATAN	22°E-31,3°E	7,5	7,3	26,5	83	6,523	884	636 E+21	98%	14,73	786	0,08	81	0,74	9	11,6	2	52	IVbaabaaa 43
	5,1°E-14°S	26,833	0,861	1,25	1,98		25 %	70%		0,18	**89,5**		**9,2**		**1**		0,23		
G5 P.KASAI	20°E-25°E	6,1	6,1	25,3	32	5,628	73	43 E+19	50%	1,22	68	0,9	3	20	2	52	0	-	IIIaaabab-11
	0,7°S-7°S		0,903	-	2,08		2,1 %	0,05%		0,04	**93**	**32**	**4**		**3**		0	-	
G6 P.BDD-BC	12°E-20°E	0	0	0			0	0	0%	0	0		0		0		0		0
	0,7°S-7°S	0					0%	0%		0	**0**		**0**		**0**		0		
G7 EQT	17°E-25°E	5,9	6,6	24,7	42	5,83	41	238 E+18	22%	0,68	28	2,1	12	5	0	-	0	-	IIabaaaab
	0,7°S-6°N	24,725	0,617	2,02	1,42		1,2 %	0,03%		0,02	70		30		0		0	-	7
G13 SOUTH	10°E-35°E	7,5	7,5		300	6,513	2321	784 E+21	100 %	38,68	2097	0,03	184	0,33	27	3,9	4	26	IVbbabab-51
	2°S-6°N		0,931	2,20	2,14		66 %	86%		0,13	**87,9**		**10,4**		**3**		0,4		
G14 NORTH	10°E-35°E	7,1	7,4		200	6,310	1205	123 E+21	100 %	20,1	1024	0,06	149	0,4	24	4,3	1	104	IVaaabbab 34
	2°S-6°N		0,916	2,5	2,10		34 %	14%		0,1	91		6,5		2,1		0,1		
G30 VICTORIA	31,5°E-36°E	7,1	7,3		23	6,27	1125	107 E+21	97%	18,8	1029	0,06	73	0,8	22	4,73	1	104	IVaabbab 38
	5°S-10°S		0,896		2,06		32 %	12%		0,82	91,5		6,5		2		0,1		

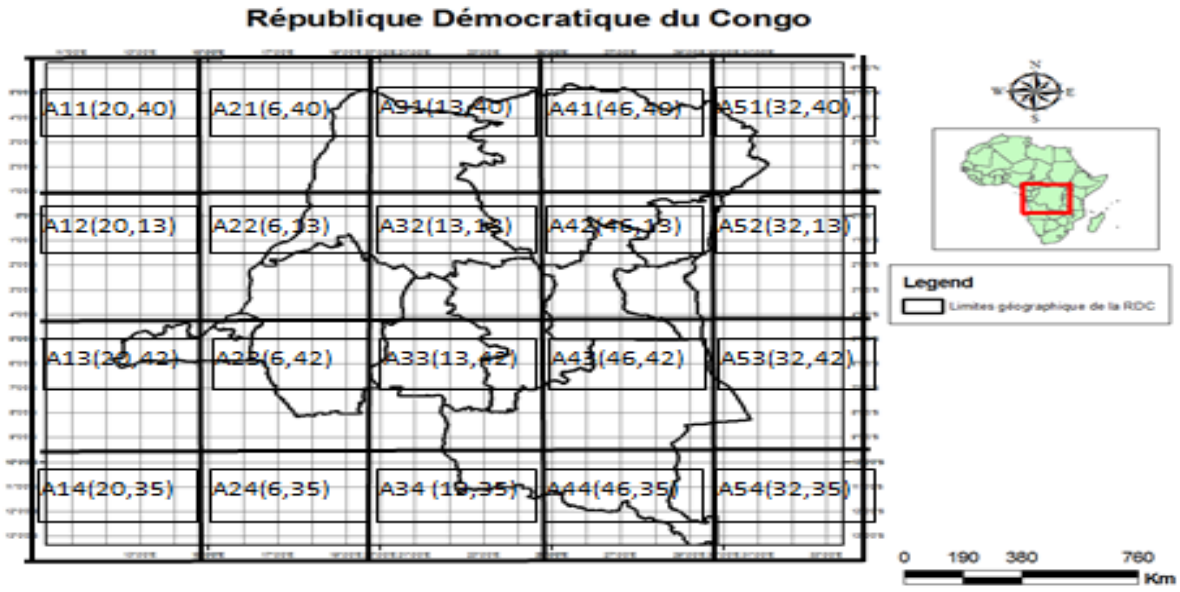

Fig. 3.4: Vertical and horizontal subdivision of the territory of the DRC and concept of Zone-Grids (Aij): grid of five square degrees

The results of the computation of the moduli of each cell deduced from the data of figure (3.4) are contained in table (3.4.).

Table 3.4a: Modulus (seismic level) corresponding to each cell.

AREA	MODULE	AREA	MODULE	AREA	MODULE	AREA	MODULE	AREA	MODULE
A11	45	**A21**	41	**A31**	42	**A41**	61	**A51**	41
A12	24	**A22**	14	**A32**	18	**A42**	48	**A52**	35
A13	47	**A23**	42	**A33**	44	**A43**	62	**A53**	53
A14	40	**A24**	36	**A34**	37	**A44**	58	**A54**	47

3.1.4. Seismic levels of Zones-Provinces and Zones-Rift

The results relating to the seismic levels of the Zones –Provinces and of Zones-Rift in figure (2.1), are contained in table (3.4b) below. These levels were obtained by classifying all the seismic species so far identified during our research across various seismic zones. This code remains "immutable" until then.

Table 3.4b: Seismic species and their corresponding levels of the Rift zones (Ri) and Zones-Provinces (Gi)

AREA	**Area Settings (1973-2008)**		**Area Settings (1910-2013)**	
	Seismic Species	**Seismic Level**	**Seismic Species**	**Seismic Level**
G1 (DRC, ALL)	IIIbbabbba	30	Ivbbababa	51
G2 (EASTERN PROVINCE)	IIIabaabbb	21	IIIababab	25
G3(KIVU)	IIIababbbb	25	IIIaaabbbb	14
G4 (KATANGA)	IIIbbababa	29	Ivbaabaaa	43
G5 (TWO KASAI)	IIaaaaaaa	1	IIIaaabab	11
G6 (BANDUNDU -)	0(Asismique)	0	0 (Asismique)	0
G7 (EQUATOR)	IIabaaaab	7	IIabaaaab	7
G8(TANGANYIKA)	IIIbbabbba	30	Ivbabbaaa	49
R1 (UPEMBA RIFT)	IIIbbabaaa	29	IIIababaaa	23
R2 (MOERO LAKE)	IIababbba	8	IIIaaabbba	13
R3 (MALAWI LAKE)	IIIbaababb	28	Ivaaababb	37
R4 (RUKWA LAKE)	IIIabbbaaa	26	IIIaabbaaa	17
R5 (TANGANYIKA LAKE)	IIIabbbbbb	27	Ivbabbaab	50
R6 (KIVU)	IIIabbbbba	27	IIIabbbbba	27
R7 (SOUTH SUDAN)	IIIbbaaaab	29	IIIabaaaab	21
R8 (NORTH ZAMBIA)	IIabaabb	8	IIaaabbb	3
R9 (ALBERT-EDOUARD LAKE)	IIIababbbb	25	Ivaabbaba	39

ISSN No:-2456-2165

3.2. Discussion of results

The discussion of the results is done according to several aspects which all highlight the advantages generated by our model; these are the following:

3.2.1. Monitoring of the seismic activity of an area: design of the acti-seismometer

Using the results of Table (3.4b) provides a means of monitoring the seismic activity of an area; this monitoring will be done according to two approaches: one called linear or Cartesian, the other called circular or polar.

3.2.1.1. Linear approach

The linear approach consists of placing the zoning level on the ordinate and the corresponding zone on the abscissa. The figure below compares most clearly the seismic activity of the areas of the DRC for two periods, namely 1973-2008 and 1910-2013.

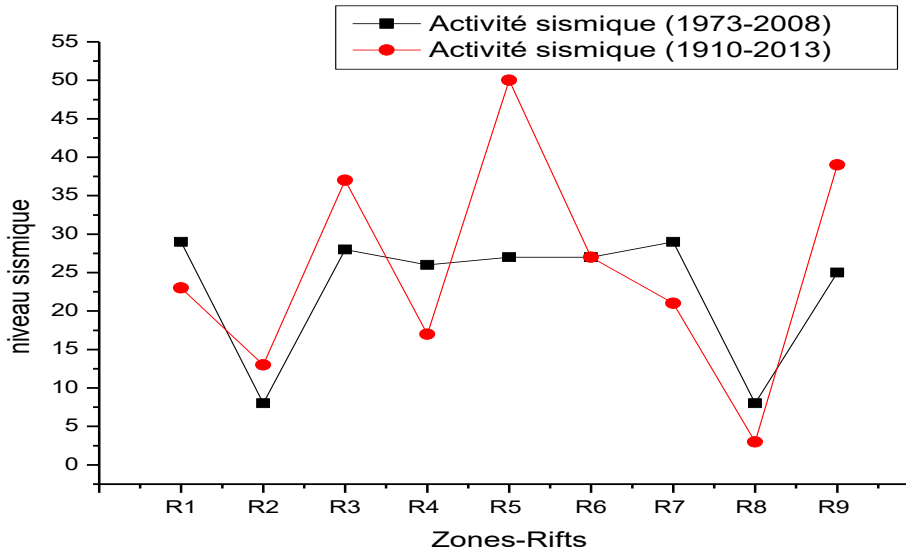

Fig. 3.5: Dynamics of the seismic activity of the zones - Rift for two periods (legend)

Similarly, the study carried out on the Pacific Coast zone of Central America (135°W-90°E; 0°-45°N), for the period from 1978 to 2013, the data of which was processed by not three years, highlights the dynamic nature of the seismic activity (Fig.3.6). For this description, we have used the match rate parameter.

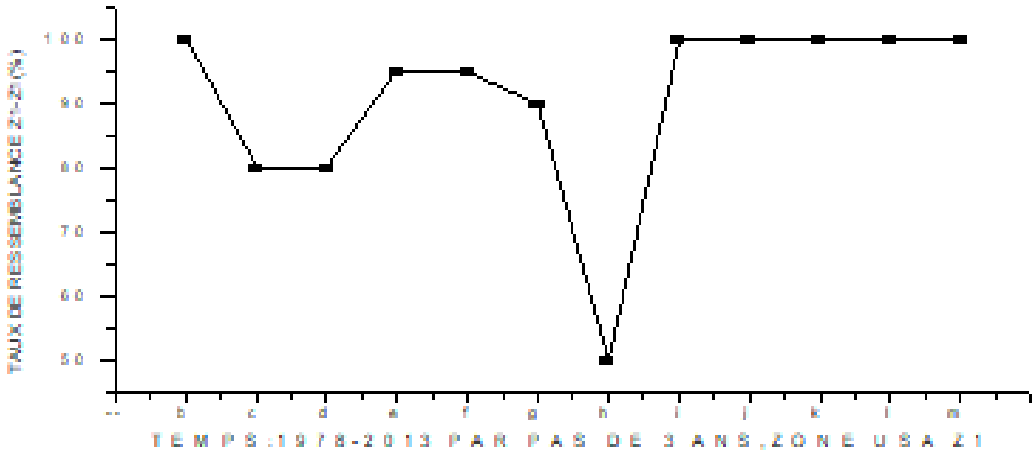

Fig.3.6: Dynamics of the internal structure of the Pacific coast zone; from 1978 to 2013 in steps of three years

3.2.1.2. Circular approach: design of the acti-seismometer

This approach consists in representing on the circumference the results of Table (3.4b) in the form of vectors, of the same origin and modulus, but of different opening angle. The transformation of the seismic levels into polar coordinates (angles), is done as follows:

We have sixteen areas to which correspond sixteen seismic levels (N_i);

The argument (angle θ_i) of each area is calculated using the following formula:

$$\theta_i = \frac{360^\circ}{16} N_i \qquad (3.7)$$

We therefore switch from the linear representation to **the vector representation** of the seismic activity of an area (Table 3.5). This last representation makes it possible to better follow seismic activity and geodynamics in the region; for this purpose, we have just developed a virtual device called **acti-seismometer**: with **"Acti",** to signify **activity** (Fig.3.7a).

Table 3.5: Transformation of seismic levels into Polar coordinates of zones for two periods

Area	Dynamic 2 (1973-2008)		Dynamic 1 (1910-2013)	
	Seismic Level 2 (N_{i2})	θ_1(°)	Seismic Level 1 (N_{i1})	θ_2(°)
R1	13	292,5	8	180
R2	4	90	4	90
R3	11	247,5	11	247,5
R4	8	180	6	135
R5	10	225	15	337,5
R6	9	202,5	10	225
R7	12	270	7	157,5
R8	3	67,5	1	22,5
R9	7	157,5	12	270
G1	15	337,5	16	360
G2	5	112,5	9	202,5
G3	6	135	6	135
G4	14	315	13	292,5
G5	1	22,5	3	67,5
G7	2	45	2	45
G8	16	360	14	315

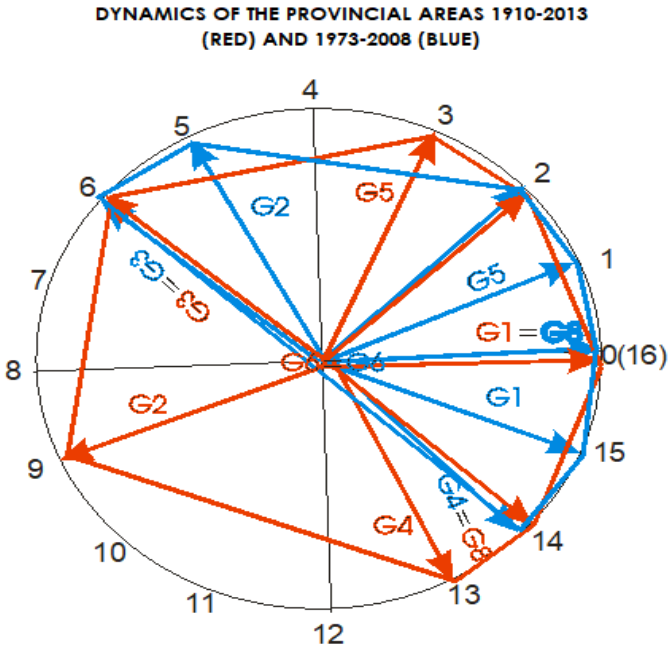

Fig. 3.7a: Vector representation of Zones-Provinces (in blue) and of the Zones-Rift (in red) using the Acti-seismometer

3.2.1.3. Characterization according to the structure-surface-perimeter and speed parameters

We are interested, for example, in the Zones-Provinces (Table 3.5). We identify their positions in terms of quadrant, level and angle for two different periods, that is to say between 1973-2008 and 1910- 2013, i.e. a time interval of 68 years. Considering the period 1910-2013 for reference or origin (initial position) of the movement and 68 for period, the speeds of the zones are obtained as follows (Table 3.6a, taken from Table 3.5):

- Linear Speed: $V_{li}=\frac{N_2-N_1}{68}$ (3.8)
-
- Angular Velocity: $\omega_{li}=\frac{\theta_2-\theta_1}{68}$ (3.9)

Table 3.6a: Vector coordinates and occupation of Zone-Provinces quadrants by period

Area	Occupied Quadrant		Position (Seismic Level, Angle)		Speed		
	1910-2013	1973-2008	1910-2013	1973-2008	Linear V_{li} Level/Year	Angular ω_{li} Degree /Year	Finding
G1	IV	IV	(16,360°)	(15, 337.5°)	-0,0147	-0,3309	Decrease
G2	III	II	(9, 202.5°)	(5, 112.5°)	-0,0588	-1,3235	Decrease
G3	II	II	(6 ,135°)	(6,135°)	0	0	Static
G4	IV	IV	(13, 92.5°)	(14,315°)	+0,0147	+0,3309	Increase
G5	I	I	(3, 67.5°)	(1, 22.5°)	-0,02694	-0,6618	Decrease
G6	I	I	(0,0°)	(0,0°)	0	0	Static
G7	I	I	(2,45°)	(2,45°)	0	0	Static
G8	IV	IV	(14,315°)	(16,360°)	+0,0294	+0,6618	Increase

The position of each zone vector in figure (3.7a) brings us to the notion of structure, area, perimeter and rate of change of the structure.

By structure, we mean the polygon obtained by successively connecting the ends of the vectors of figure 3.7a; this polygon is characterized by its shape, area and perimeter, the evolution of which can be followed over time and therefore the geodynamics of the area (Figure 3.7.a). By calculating the speed V_S of the surface (S) or V_P of the perimeter (P), we obtain:

$$\frac{P_f}{P_i} = \mathbf{0,844} \quad \textbf{(3.10)}$$

$$\frac{S_f}{S_i} = \mathbf{0,570} \quad \textbf{(3.11)}$$

$$\Delta S = S_f - S_i = -1,084\ U \quad \text{and} \quad V_S = -0,0159\ U/\text{year} \quad \textbf{(3.12)}$$

and $$\Delta P = P_f - P_i = -8,2\ U \text{ and } V_P = -0,1206\ \text{U/year} \quad \textbf{(3.13)}$$

From the calculation of these parameters, the following results:

• We note that the surface, the perimeter and their respective speeds, have decreased; thus we have just quantified the geodynamics of the Zones-Provinces of the DRC between two given instants. We say that the seismic activity was stronger in the period 1910-2013 than in that of 1973-2008,

• We note, moreover, that if certain vectors-zones have conserved the position in the quadrant, it is not the case for others: certain zones have increased in level (positive speed) while others have decreased (negative speed). These observations appear in the last column of the table (3.6a).

3.2.1.4. Characterization according to the reduction of the quadrilateral structure

The reduction of the structure consists first of transforming the polygon into a quadrilateral; which amounts to finding the resultant of the vectors-zones of each quadrant. On the basis of the results of Table (3.6a), we obtain the table and figure below.

Table 3.6b: Comparison of the results of the Zones-Provinces according to the position of the vectors.

Quadrant	Cartesian Coordinates				Polar Coordinates			
	1910 – 2013 (Gi)		1973 – 2008 (Gi)		1910 – 2013 (Gi)		1973 – 2008 (Gi)	
	Abscissa	Ordinate	Abscissa	Ordinate	R (module)	θ (angle)	R (module)	θ (angle)
I	1,09	1,631	1,631	1,091	1,964	56°	1,964	34°
II	-0,707	0,707	-1,09	1,631	1	146°	1,964	135°
III	-0,924	-0,384	0	0	1	202,5°	0	0°
IV	0,383	-0,924	0,707	-0,707	1	292,5°	1	315°

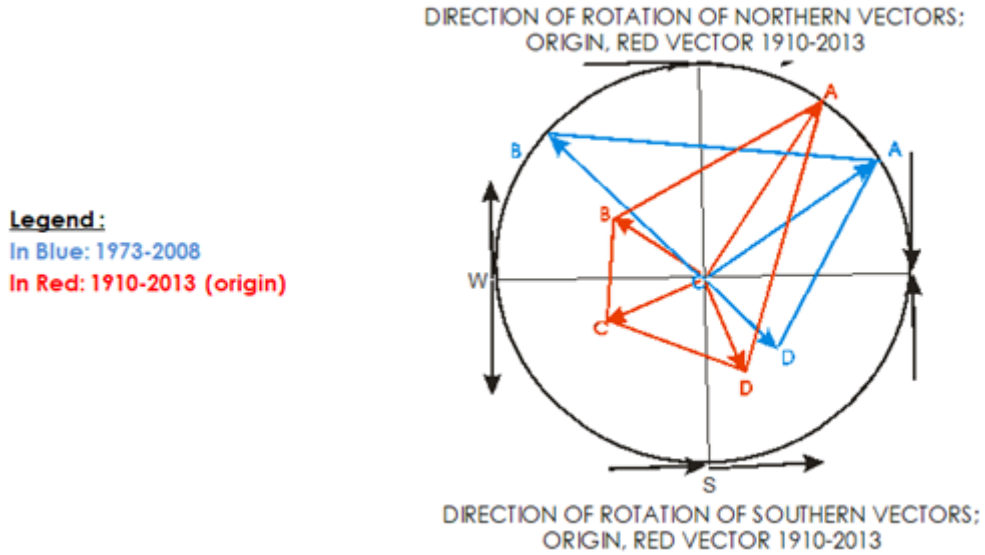

Figure 3.7 b: Dynamics of the seismic activity of the DRC through the reduced structures of the Zones-Provinces

Proceeding as later, the results look like this:

$$\frac{P_f}{P_i} = 1,282 \quad (3.14)$$

$$\frac{S_f}{S_i} = 1,057 \quad (3.15)$$

$$\Delta S = S_f - S_i = +1,45\ U \text{ and } V_S = +0,0217\text{U/year} \quad (3.16)$$

$$\text{and} \quad \Delta P = P_f - P_i = +6,1\ U \text{ and } V_P = +0,0897\text{U/year} \quad (3.17)$$

We can also calculate the angular variation of each vector resulting from the quadrant from the displacements of points A, B, C and D in figure (3.7b).

The total relative angular variation , α_t, sum of all variations, is worth:

$$\alpha_t = +\alpha_{AA} + \alpha_{BB} + \alpha_{CC} + \alpha_{DD} = +12° \quad (3.18)$$

and the relative speed of rotation, $\omega_{\alpha t}$, is worth:

$$\omega_{\alpha t} = +0,1765°/year \quad (3.19)$$

From these results, we draw the following summary observations:

- The 1973-2008 and 1910-2013 structures are not identical; the sensitivity of the model therefore makes it possible to follow the seismic activity wonderfully through the quantified variations in shape and position of structures and vectors,
- Taking as origin the period 1910-2013, we note that the points of the northern hemisphere (A and B) rot in the trigonometric direction, that is to say from right to left, while those of the southern hemisphere (C and D) rotates in the opposite direction:
- While two sides having a common point contract (BC and BA), two others expand (CD and DA).

The Figure below compares the dynamics between reduced structures of Zone-Provinces (top) and Zones-Rift (bottom) for two periods, (1910-2013) and (1973-2008); two main observations follow from this:

- Compared to their respective signs, the speeds of the Zones-Provinces are of opposite signs to those of the Rift zones: indeed, we note, for example, that when the points A and B of the Zones-Provinces turn clockwise. 'a watch is the reverse for Rift Zones,
- While sides $\overline{BC}>\overline{BC}$, $\overline{AB}>\overline{AB}$ et $\overline{CD}<\overline{CD}$, $\overline{DA}>\overline{DA}$ in Zones -Rift, c t is the opposite which occurs in the Zones-Provinces.

ISSN No:-2456-2165

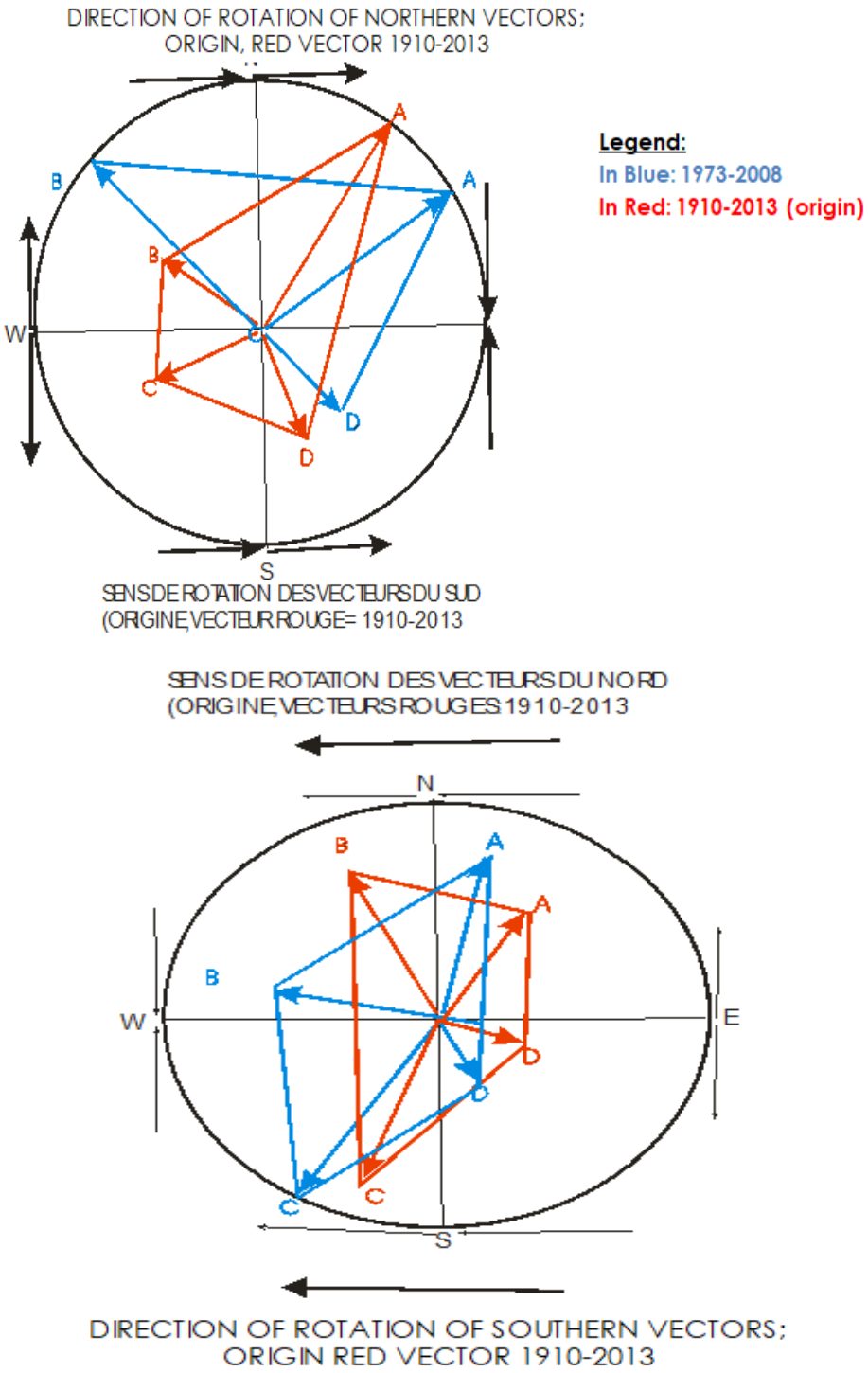

Figure 3.7c: Comparison of the dynamics between reduced structures of Zone-Provinces (top) and Zones-Rift (bottom)

3.2.2. Characterization of seismicity using curves

The results of Table (3.4) have been transformed into curves (Fig. 3.8), the whole of which characterizes the structure of a seismic zone; we call it signature or imprint of the affected area. This signature can be tracked in time and space: two seismic zones with the same signature are identical (in terms of seismic activity, or even geological structure). Which could serve us for geological prospecting. Each point on the curve represents a mesh Aij whose modulus (seismic level) is read on the ordinate.

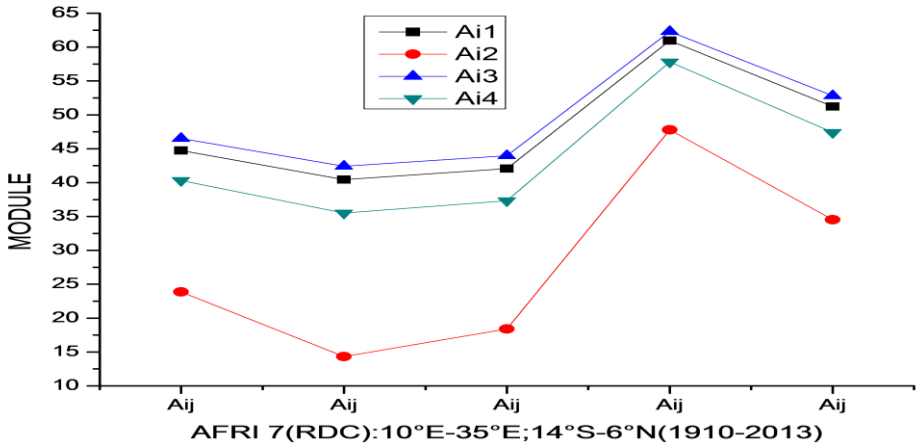

Fig 3.8a: Graphic characterization of the seismicity of the DRC (1910-2013)

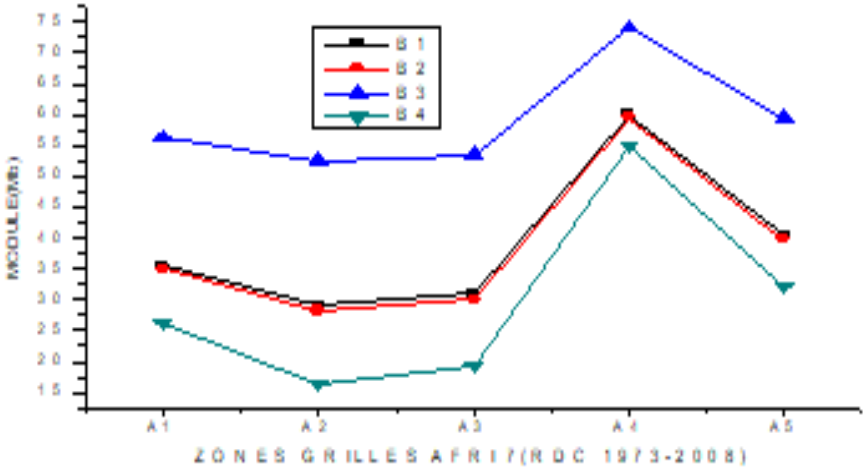

Fig3.8b: Graphic characterization of the seismicity of the DRC (1973-2008)

Observation of these curves indicates that :

- The DRC's seismicity is diversified both from West to East and from North to South, but it is however very intense towards the Rift zones (in the East of the country);
- These curves show a clear distinction between the Rift zones with high seismicity and those outside the Rift with weak seismicity; the limit between these two zones is located at 25°E.
- The comparison of these graphs (Fig.3.5a and 3.5b) shows the following :

➢ The global structure of the seismicity is preserved for the two periods; a lull in the Congolese craton opposed to intense activity in the rift zones,

➢ A difference in seismic levels: the maximum level is 75 for the period 1973-2008, while it is 65 for the other period (1910-2013).

3.2.3. Comparison of the seismic activities of two zones using an equation

The figures above, for example figure (3.8a), make it possible to establish a mathematical relationship between the curves traversing the meshes horizontally: Thus, we will have for example the following equations:

$$Y_{L3} - Y_{L1} = +2,5 \quad \text{or,} \quad Y_{L3} = Y_{L1} + 2,5 \qquad (3.20)$$

$$Y_{L3} - Y_{L4} = Y_{L4} + 7,5 \quad \text{or,} \quad Y_{L3} = Y_{L4} + 7,5 \qquad (3.21)$$

$$Y_{L3} - Y_{L2} = +22,2 \quad \text{or,} \quad Y_{L3} = Y_{L2} + 22,2 \qquad (3.22)$$

Where is the value of the seismic level read on the y-axis for the nth horizontal band (line) in the figure above; each horizontal band is symbolized in the legend by Ai1,…, Ai4. In figure (3.8.a), L1, L2, L3, L4 are respectively indicated in black, red, blue and green.

The difference in zoning levels, also called Shift, between the two curves is clearly deduced on the y-axis.

3.2.4. Characterization of the internal structure or seismic profile (tomography)

3.2.4.1. Introduction

The internal structure or seismic profile of a zone consists in drawing the curve which indicates the variation of the seismic level as a function of the depth for each Aij cell and for each depth slice (Table 3.7; Fig. 3.12-15). By assigning a color code to the results of Table (3.4) we obtain a zoning map of the internal structure of the area, also called tomographic (Fig. 3.13; 3.15-16).

Table 3.7: correspondence between layer and depth slice (Fig.3.1)

Areas-depth	Meaning	Depth (km)	Longitude (°)	Latitude (°)
G1	**G**ranite Layer **1**	0-5	10E-35E	14S-6N
G2	**G**ranite Layer **2**	5-10	10E-35E	14S-6N
G3	**G**ranite Layer **3**	10-15	10E-35E	14S-6N
G4	**G**ranite Layer **4**	15-20	10E-35E	14S-6N
B1	**B**asaltic Layer **1**	20-25	10E-35E	14S-6N
B2	**B**asaltic Layer **2**	25-30	10E-35E	14S-6N
B3	**B**asaltic Layer **3**	30-35	10E-35E	14S-6N
B4	**B**asaltic Layer **4**	35-40	10E-35E	14S-6N
SM1	Layer Under Coat **1**	40-105	10E-35E	14S-6N
SM2	Layer Under Coat **2**	105-170	10E-35E	14S-6N

3.2.4.2. Characterization using curves

The calculation of the seismic level at each depth slice is presented in figure (3.9)

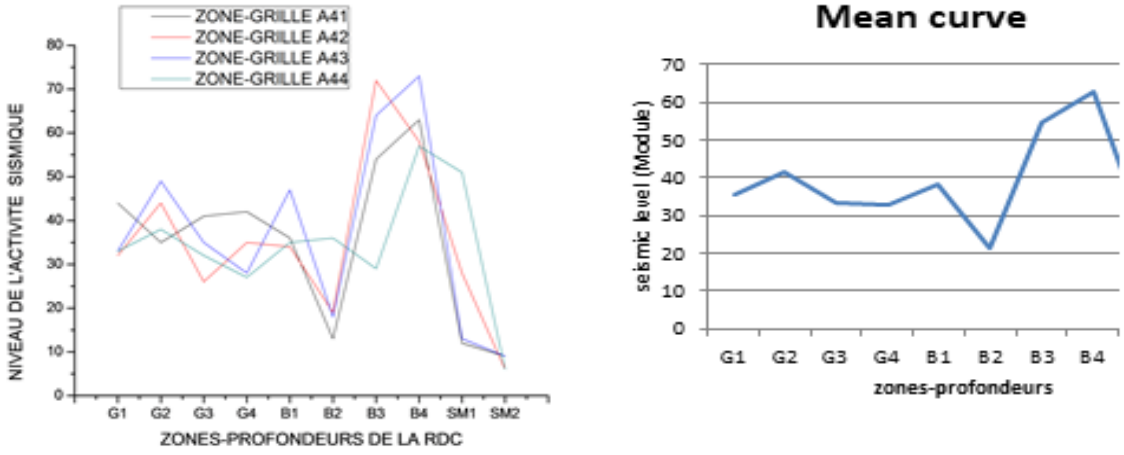

Fig. 3.9: Dynamics of seismic activity in the DRC as a function of depth

Observation of the average curve (right) indicates that the structure is subdivided into two:

- The granite layer (G1-G4): it is characterized by a line of decreasing slope modeled by figure (3.7) on the left,
- The basaltic zone (B1-B4) to the sub-mantle zone (SM1): the structure is characterized by a concavity parabola turned downwards, the axis of symmetry of which is located at B4 (on the abscissa) with a seismic level maximum of 67 (on the y-axis),

Observation of figure (3.9) on the left highlights an important fact: it shows that the A43 (Tanganyika) and A42 (Kivu) zones have the same pace, but paradoxical at B4 (35-40km). Indeed, at this place we observe that the seismic level increases for A43, while it decreases for A42. This fact could be justified by the difference of the structures at these places, due in particular to the difference of the depths of these two lakes, the structure of faults and the presence of volcanoes (for A42, Nyiragongo volcano, Nyamulagira, see Figure (3.22): Ngindu,2021,Wafula,2009 ; Zana and al.,1981).

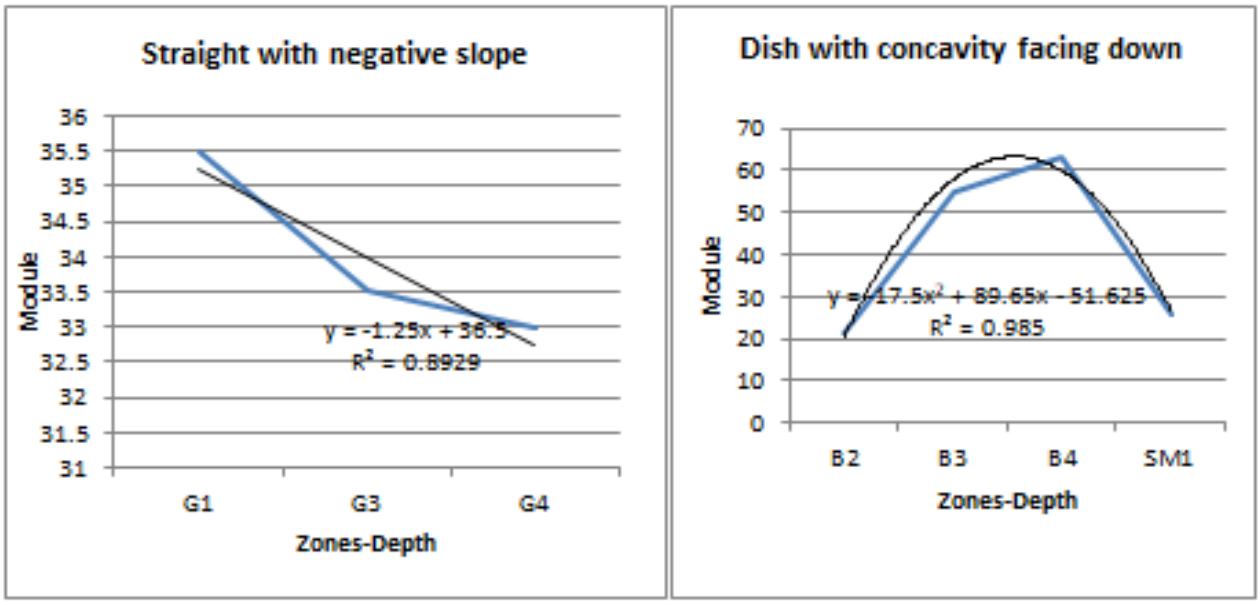

Fig. 3.10: Modeling of the average curve characterizing the internal structure of the DRC.

In addition, we were interested in the analysis of the most active zone, located in the Rift-Congolais, in particular the fourth column (25°E-30°E). This area includes stitches A41, A42, A43 and A44 (Fig.3.4).

We calculate two parameters there; the Ratio and the Gradient of the seismic level:

- **The ratio**

We define the Ratio (Rij) as being the ratio of two seismic levels (Ni and Nj, with j = i + 1) of successive depth zones. "I" and "j" refer to the layer (Gi, Bi or SMi), hence:

$$R_{ij} = \frac{N_j}{N_i} \qquad \textbf{(3.23)}$$

The results of this relation are expressed by figure (3.8) and indicate :

- An overall ratio greater than unity (1), meaning that the seismic activity increases with depth,
- A very high Ratio at SM1 (40-107km) for zones A42 (Zone Kivu) and A44 (Rift Zone of Upemba / Haut-Katanga). Structurally speaking, in these places, the faults are complex for these areas (Fig. 3.22-23),
- An almost identical behavior for zones A43 (Tanganyika zone) and A41 (South Sudan zone), because we observe that their curves are almost identical, synonymous with a structural identity.

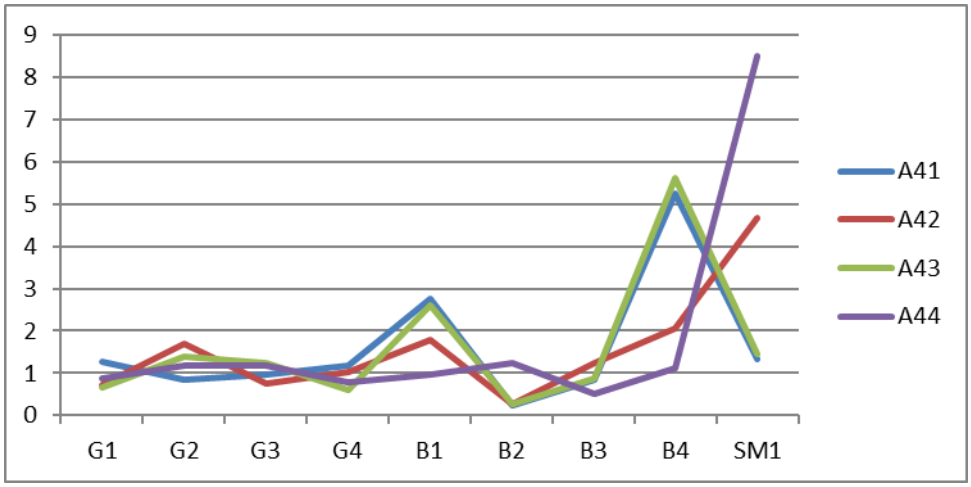

Fig. 3.11: Dynamics of the ratio of seismic activity as a function of depth

- **The Seismic Level Gradient**

The Gradient (Gij) of the seismic level is defined as being the ratio between the difference of the seismic levels (Ni and Nj, with j = i + 1) of two successive depth zones and the difference of their distance (Dji). From where :

$$G_{ij} = \frac{N_j - N_i}{D_j - D_i} \quad \textbf{(3.24)}$$

Applying this relationship to the results provides the curves below which indicate, on the one hand, a structure subdivided into three parts, all of which are wave-shaped :

- **The granite part (G1-G4):** here, the amplitude of the seismic levels of the curves varies in the interval [-20, + 20]; therefore a positive difference from the peaks of +40,
- **Most basaltic** (G4-B3), the amplitude of the seismic levels of the curves varies in the interval [-20, +50]; therefore a positive difference from the peaks of +70,
- **Most of the sub-basaltic layer** (B3-SM2), the amplitude of the seismic levels of the curves varies in the interval [10, -60]; therefore a negative difference from the peaks of -70. This translates to a stability of the structure seismically speaking.

We observe, moreover, the following:

- Zones A43 (Tanganyika zone) and A41 (South Sudan) behave almost identically,
- A somewhat peculiar behavior can be observed for zone A44, located at Lake Rukwa, in Malawi. This behavior could be explained by the fact that in this area, the faults have a different orientation (vertical, on average) from that of the others (Fig. 3.23) and that the hypocenters are deeper there than elsewhere,
- Overall, this gradient increases with depth, with a paroxysm at B2 (25-30km),
- In short, the result of these observations can be described by the curve in red represented by the Kivu zone (A42): it is on average a Gaussian whose peak is 50 and is located at B2 (25-30 km). its band width is 5km. Indeed, figure (3.23) indicates the presence of crossed faults, that is to say, both of NE-SW and NW-SE orientation.

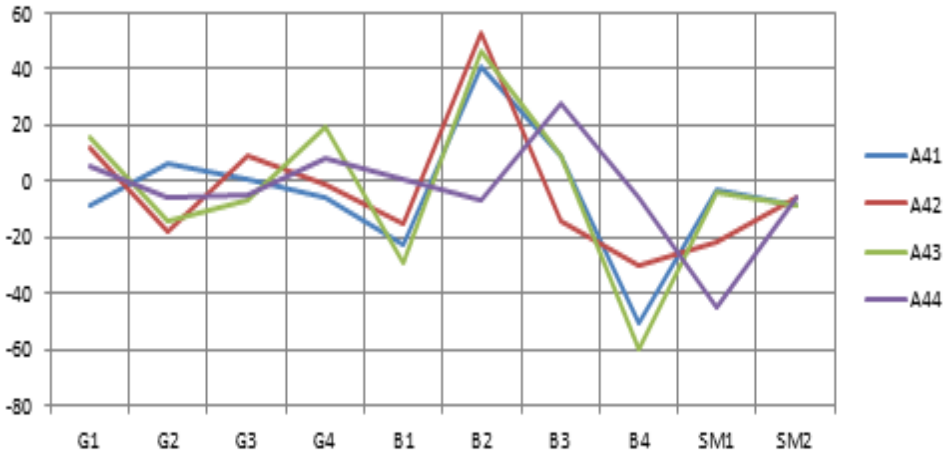

Fig. 3.12: Dynamics of the gradient of seismic activity as a function of depth.

In short, we say that the careful interpretation of the above parameters reveals the structural differences in various seismic zones studied. And could lead to geological prospecting.

Ultimately, we say that the seismicity of the DRC is better distinguished longitudinally and in depth, that is to say that there is a clear demarcation between the seismicity of the western and eastern part of the DRC than otherwise and that the behavior of this seismicity is not identical according to the depth; one Depth-Zone may not look like another.

3.2.4 3. Characterization using zoning maps: seismic tomography

The results of Table (3.4) and Figure (3.4) can be translated in the form of a map for each zone-depth and Aij cell by using a legend (Table 3.8). which results in figure (3.13). This figure shows the structure of each layer (G1-G4, B1-B4 and SM1-SM2). The map in the lower right corner shows the overall situation of the DRC, that is to say that we have taken into account all the earthquakes (from G1 to SM2).

Table 3.8: Legend relating to the zoning map (seismic structure).

Seismic level (Module)	14-18	19-24	25-33	34-44	45-58	59-77
Ladder	N1	N2	N3	N4	N5	N6
Color Code	Purple	Blue	Green	Yellow	Orange	Red

The observation of Figure (3.13), based on the contrast of colors, highlights the following :

- The difference is not remarkable between the northern part (first two lines) and the south (last two lines)

- The seismicity marks a clear difference between the zones of the rift (25-35 ° E), of strong activity and those outside the rift (10-25 ° E), of weak activity; however, the C3 zone (20-25 ° E), especially in the Upemba rift in South Katanga (A33) constitutes a suture zone (transition) between the two(Ngindu, 2021),
- Zones A22, A21 and A12 are seismically stable (low level) and located in the sedimentary zone (Congolese craton) where geophysical research has revealed the presence of hydrocarbons ((Biliki and al.,2021 ; Tondozi, 2018),
- The DRC map (lower right corner) looks like B3 and B4, which means that the DRC seismic activity is dictated by these areas (30-40km),
- Nevertheless, the part of the rift presents certain nuances:

➢ At layer B3 (30-35km), the seismic level is high in zones A42, A43, A52 and A53,
➢ At layer B4 (35-40km), it is high in zones A43 and A53,
➢ At the SM1 layer (40-105 km), the seismic level drops to be remarkable only at the L4 (14°S-9°S) and C5 (30°E-35°E) bands, precisely at the zone A54 (in Malawi, in lakes Rukwa and Malawi; Fig. (1.2)),

- From the previous observation follows the conclusion that the seismicity of the rift migrates and the hypocenters increase overall from North to South.

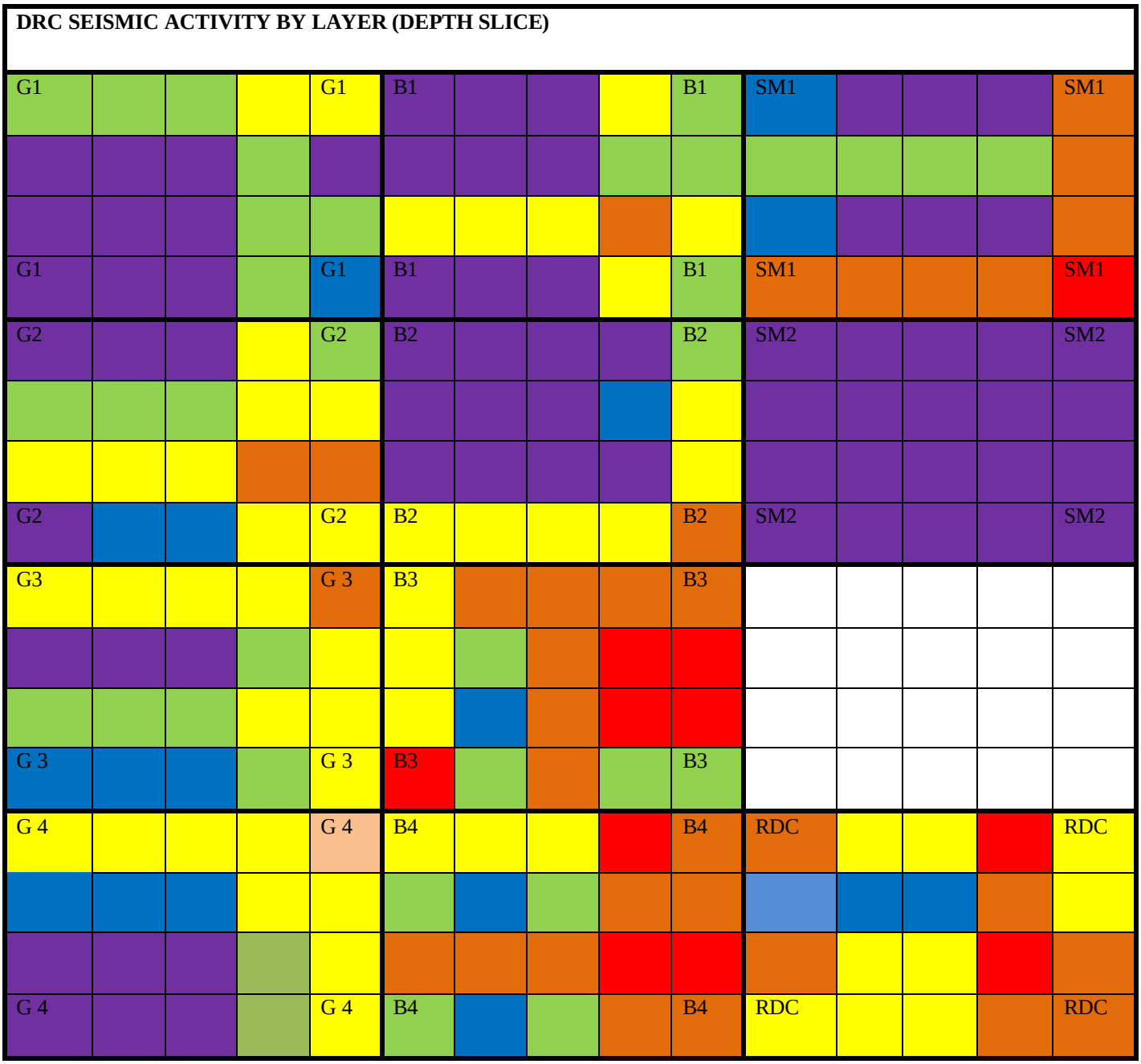

Fig. 3.13: Seismic structure of the DRC by depth section and by Aij cell

3.2.5. Comparison of areas using the match rate

For each Aij cell and for each depth slice, calculate the seismic species $\mathbf{X_{123456789}}$. The likeness rate is calculated by taking the species from layer G1 of each column or row as a reference to other layers. From the legend of the table below we draw the maps (Fig. 3.14-15).

Table 3.9: Legend relating to the similarity rate

Similarity Rate	Color
0%	
] 0-25]	
] 25-50]	
] 50-75]	
] 75-100[	
100	

AREA-DEPTH	C1 RDC (10°E-15°E)	C2 RDC (15°E-20°E)	C3 RDC (20°E-25°N)	C4 RDC (25°N-30°N)	C5 RDC (30°N-35°N)
G1					
G2					
G3					
G4					
B1					
B2					
B3					
B4					
SM1					
SM2					

Fig.3.14: describes the soil structure from the resemblance rate going from the west to the east of the DRC following the depth.

Figure (3.14) shows the difference between the seismicity of the West of the DRC (C1, C2, C3 = 10 - 25°E) and that of the East (C4 and C5 = 25-3° E).

In this case, we observe that the hypocenters become more and more superficial going from C1 to C2 (non-Rift zones) and, beyond that, the depth increases (C4 and C5, Rift zones). Nevertheless, it appears that the C3 zone (20-25°E) constitutes a transition zone between the two: this observation is justified by the presence of the colors blue and orange on the one hand and, on the other hand, following the shallower depth of hypocenters recorded there.

ISSN No:-2456-2165

Figure (3.15) describes the soil structure from the resemblance rate going from the North to the South of the DRC following the depth.

AREA	L1 DRC (6°N-1°N)	L2 DRC (1°N-4°S)	L3 DRC (4°S-9°S)	L4 DRC (9°S-14°S)
G1				
G2				
G3				
G4				
B1				
B2				
B3				
B4				
SM1				
SM2				

Fig. 3.15: Evolution of the internal structure as a function of the resemblance rate going from north to south of the DRC.

Figure (3.15) highlights the almost identical nature of the DRC's seismicity by traversing it from North to South. Consider the horizontal bands L2 (1°N - 4°S near the equator).

This band is made up of Meshes A12, A22, A32, A42 and A52. Let us follow the dynamics of each of these Meshes as a function of the seismic level (modulus) at each depth (Fig.3.16). We can note the following:

- Grid Zones A12, A22 and A32 behave in the same way at each depth,
- Grid Zones A42 and A52, on the other hand, even if the shape of their curves are the same, nevertheless, they do not have the same value of the seismic level at each depth.
- One Depth-Zone may not look like another: G1 = B1 = B4, G2 = B3, G4 = SM1. Depth G1 (0 - 5 km) corresponds to a sedimentary layer at A22 and A32 (Fig.3.4).

Gravimetric and geomagnetic surveys in these areas have revealed the presence of hydrocarbons ((Biliki and al. ,2021).

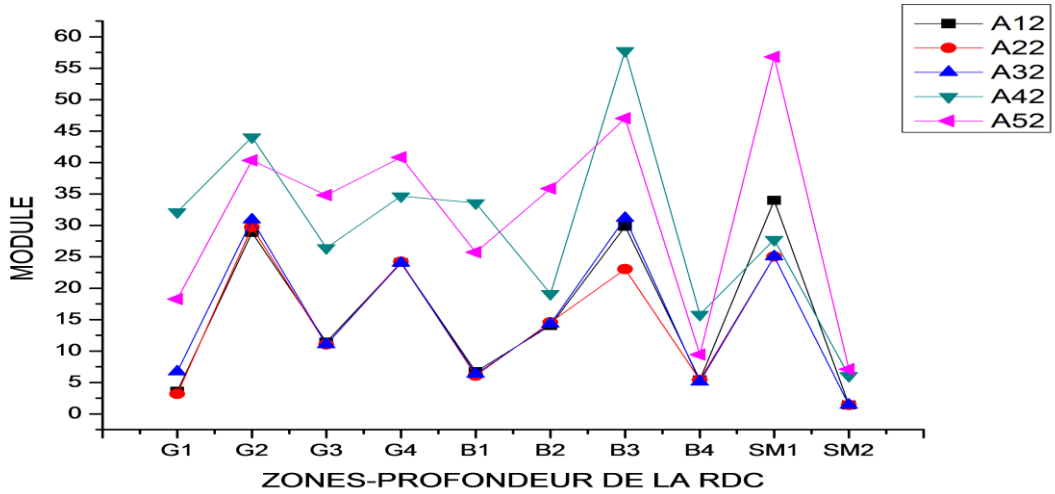

Fig. 3.16: Evolution of the seismicity of the grid zones of the second horizontal band (1°N -4°S) as a function of the depth

Ultimately, we say that the seismicity of the DRC is better distinguished longitudinally and in depth, that is to say that there is a clear demarcation between the seismicity of the western and eastern part of the DRC; this distinction is not obvious in terms of north and south (latitude). However, the zone located between 20 and 25°E constitutes a suture or transition zone between the non-Rift zone and the Rift zone.

3.2.6. Monitoring of seismic activity

The results of Table (3.4) and Figures (3.4a-b) therefore highlight the dynamic nature (in time and in space) of the seismic activity of an area. The evolution of the seismic level makes it possible to follow the geodynamics of an area over time:

The figure below compares most clearly the seismicity of the areas of the DRC for two periods, namely 1973-2008 and 1910-2013.

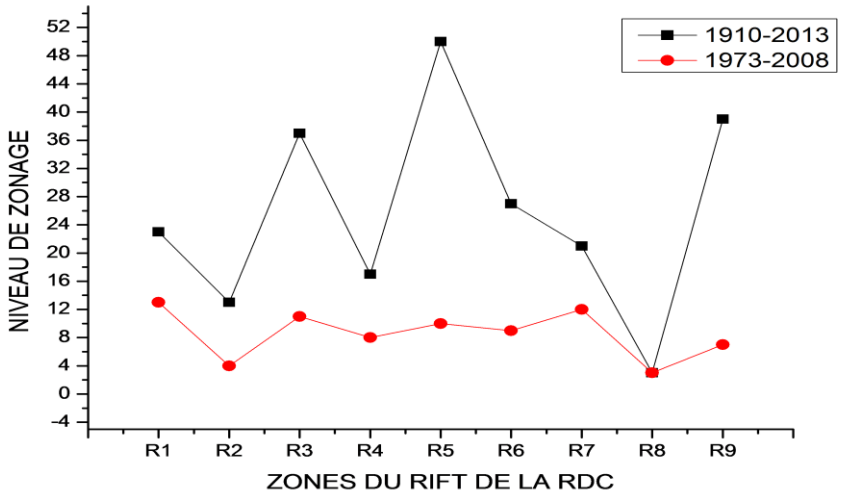

Fig. 3.17: Dynamics of the zoning level of the zones - Rift for two periods in legend

Likewise, the study carried out on the Pacific coast of Central America (135°W-90°E; 0°-45°N), for the period from 1978 to 2013, the data of which was processed by step of three years, highlights the dynamic character of the seismic activity (Fig.3.9). The resemblance rate parameter was used for this description.

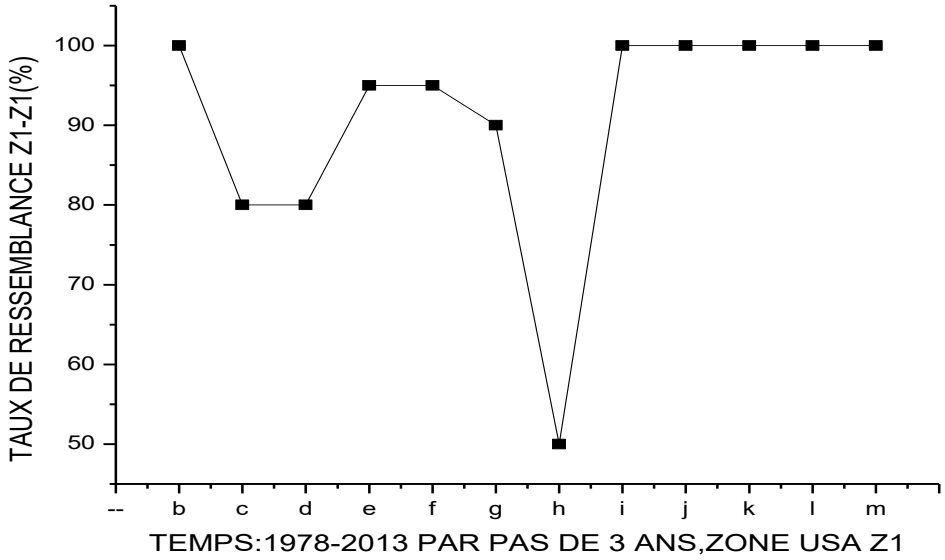

Fig.3.18: Dynamics of the internal structure of the Pacific coast zone; from 1978 to 2013 in steps of three years.

3.2.7. Analytical description of an area based on others

The scale also makes it possible to characterize a zone as being a combination of the parameters of several other zones partially identical to. We assign in front of the zone the partial resemblance rate of with respect to the zone while indicating in parenthesis, after the resemblance parameters The sum of all is 100%; hence the writing :

$R_i = \sum_{j=1}^{n} a_j R_j$ **(3.24)**

Consider the areas listed in the table below.

Table 3.10. : Seismic species of the Rift zones, 1910-2013.

Area	**Level**
R1(Upemba)	IIIababaaa
R2 (lake Moéro)	IIIaaabbba
R3 (Lake Malawi)	IVaaababb
R4 (Lake Rukwa)	IIIaabbaaa
R5 (Lake Tanganyika)	IVbabbaab
R6 (Lake Kivu)	IIIabbbbba
R7 (Sud-Soudan)	IIIabaaaab
R8 (Nord-Zambie)	IIaaabbba
R9 (Lake Albert-Edouard)	IVaabbaba

By way of illustration, the application of the principle on the calculation of the rate of resemblance to the results contained in the table above makes it possible to write (Mukange, 2021a):

100(%)R4(X,1,2,3,4,5,6.7)=75(%)R2(X,1,2.7)+25(%)R5(3,4,5,6) (3.25)

100(%)R5(X,1,2,3,4,5,6,7)=75(%)R3(X,1,3.7)+10(%)R7(5.6)+15(%)R2(2.4) (3.26)

3.2.8. Seismic risk assessment

Applying the model designed to our results, leads to the establishment of the maps below (Mukange, 2021a)).

ISSN No:-2456-2165

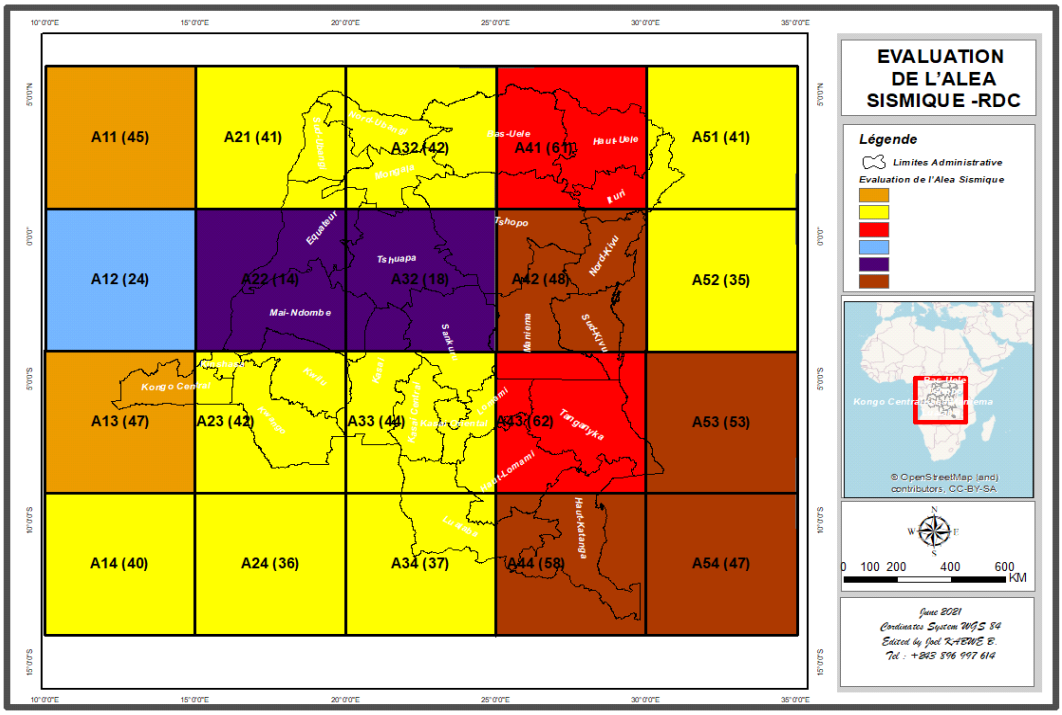

Fig. 3.19: Seismic hazard assessment map using the module (seismic level, in brackets)

The above seismic hazard map has been developed according to the model which considers a seismic zone Aij as a vector whose components take into account the seismic level of the column and the line which constitute it. This results in the attribution of a seismic level to any zone, even if it is not classically; case of the Kinshasa-Bandundu (A23), Kongo-Centrale (A13) Zone…. However, their environment records earthquakes (Fig.1.1).

Ideally, to reduce this seismic level in areas conventionally considered to be seismic, it would be to reduce the dimensions of the meshes and of the main zone subdivided into Aij mesh. For example, work on a square area of side 10 degrees (instead of 25° times 20° as is the case) subdivided into square meshes of side 2 degrees each (instead of 5° currently)

Let us use the results of the Table below, and others (Mavonga, 2009 ; Bantidi, 2014), which have made it possible to establish the correlation between the attenuation of the intensity of an earthquake and the epicentral distance from the Kabalo / DRC earthquake (Mukange, 2015):

Table 3.11: Relationship between Intensity (I = y) and epicentral distance (R = x, in km).

N°	Direction	Right : $I = aR + b$ Or $Y = ax + b$	a	$Xmax = -\frac{b}{a}$
1.	Kabalo-Goma Axis	$y = -0{,}011x + 8{,}282$	0,011	753
2.	Kabalo-Moba Axis	$y = -0{,}009x + 7{,}370$	0,009	819
3.	Kabalo-Lubumbashi Axis	$y = -0{,}006x + 7{,}616$	0,006	1269

These results indicate that any earthquake occurring at an average distance of more than 1269 km will never be felt in areas A23, A22 and others. However, we had to record major earthquakes (magnitude 6 and more) in the part between 10°E and 15°E (Fig.1.2), less than 500km from Kinshasa (A23), in Gabon (A22). Recall that we note the presence of a nuclear power plant in Kinshasa.

We therefore want to say that, although the seismic hazard in zones A23, A22 and A13 are required by our scale, at least by exploiting the attenuation curve of the Kabalo-Lubumbashi axis (Table 3.11), we find a seismic intensity of 5 for an earthquake that can occur at a distance of 500km from Kinshasa. However, the seismic hazard in this area can be revised downwards and would drop from A23 (42) to A23 (24). In fact, the level of seismic risk must also be reduced there.

ISSN No:-2456-2165

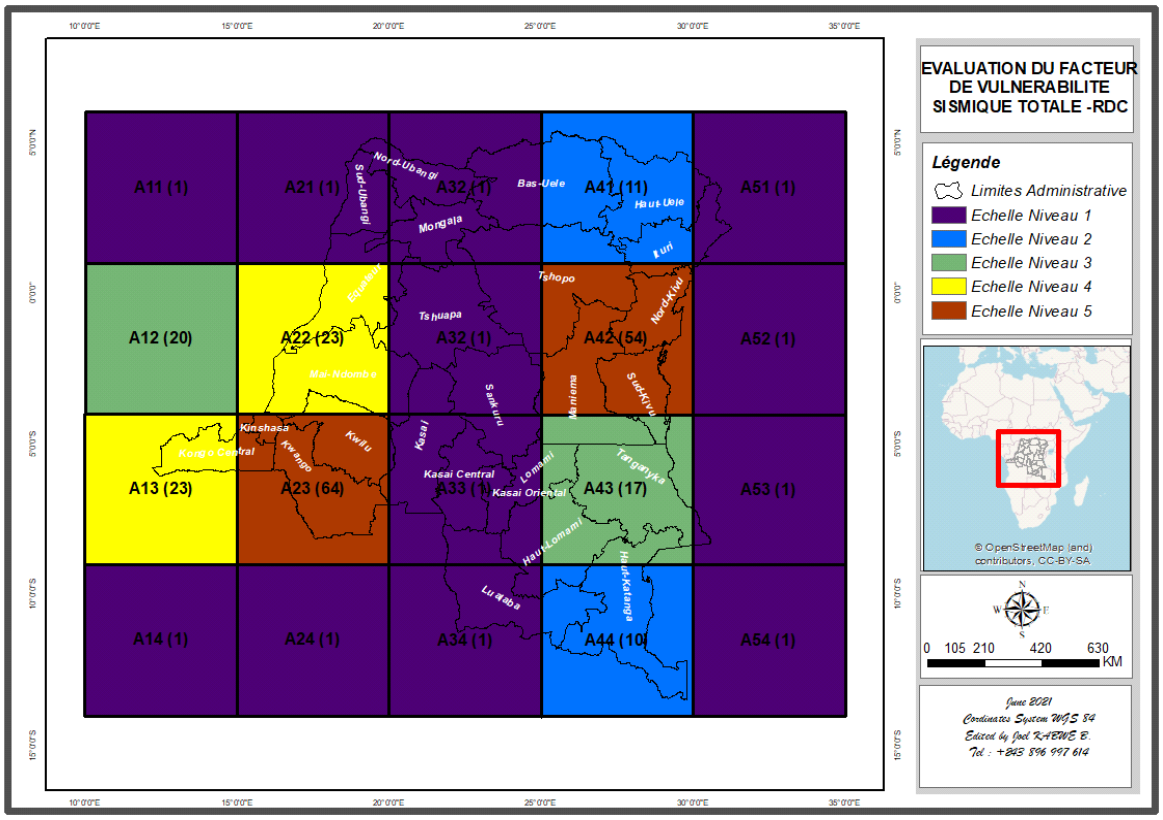

Fig. 3.20: Vulnerability factor assessment map (vulnerability scale brackets)

As for the map above, which consists of evaluating the vulnerability factor (Fig. 3.19), our scale took into account two factors, one called sociological (population density, level of infrastructure and structures, capacity risk management,… ..), the other called environmental factor (presence of a volcano, a lake, nuclear power plant and their combination). Combined, these Factors estimated high values of the vulnerability factor in the following areas :

- **Zone A23** (Kinshasa-Bandundu and surroundings), following:
  - The presence of the Kinshasa nuclear power plant, the danger of which is not negligible in the event of an accident (Muswema, 2015),
  - The presence of the Atlantic Ocean where minor earthquakes are recorded (Fig.1.2),
  - The presence of faults observed there (Fig.3.23), not to mention the high density of the population.
- **Zone A42** (Kivu): here, this factor is important due to:
  - The presence of volcanoes (Nyiragongo, Nyamulagira….) Whose flow is heading towards the city(Wafula, 1999, 2009,2011),
  - The presence of Lake Kivu containing harmful gas (methane gas and carbon dioxide; Zana, 2010),
  - The presence of complex faults observed there as well as the high density of the population (Fig.3.22-23).

Associating the seismic hazard with the vulnerability factor, using the logarithmic scale (Mukange, 2021a), we obtain the map evaluating the seismic risk in each Aij zone of the DRC.

ISSN No:-2456-2165

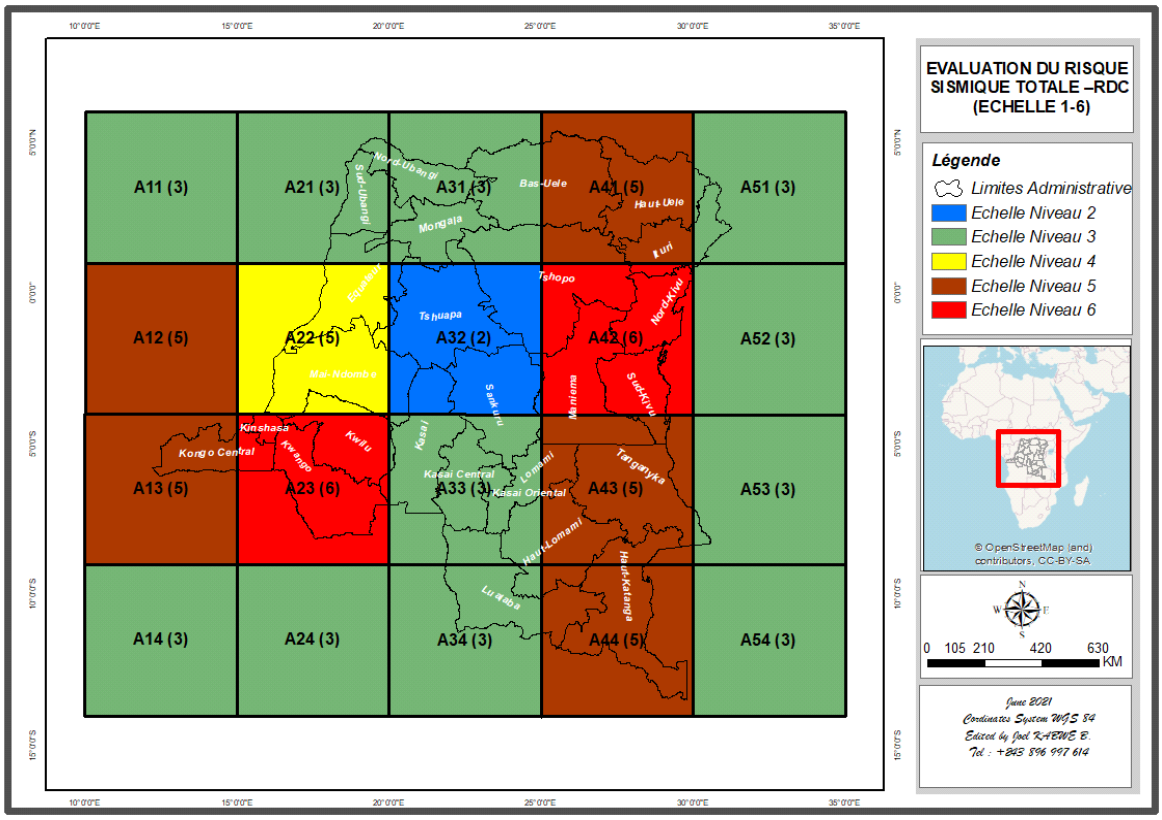

Fig. 3.21: Seismic risk assessment map in the meshes (logarithmic scale in brackets)

Taking into account the above observations relating to the reassessment of the seismic hazard in zone A23 with an impact on the level of seismic risk, it changes from red to orange. In this case, only the Kivu zone (A42) presents the highest seismic risk. However, the level of risk is still alarming that this area also deserves special monitoring(Bantidi ,2014).

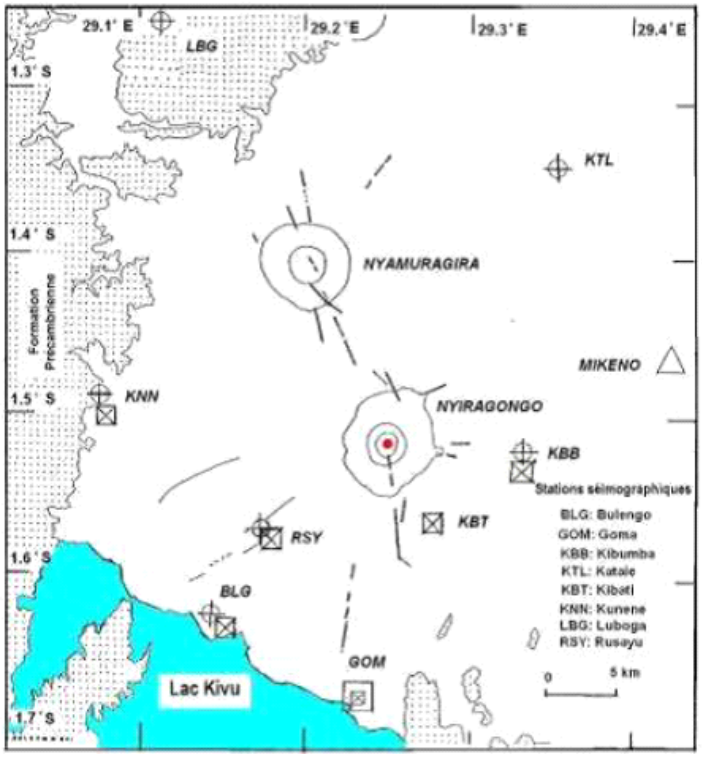

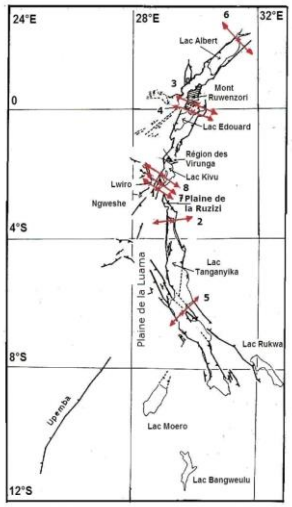

Fig. 3.22: Environment in the Kivu zone (A42), Tanganyika zone (A43) and Upemba Rift zone (A44) (Wafula ,2009).

ISSN No:-2456-2165

These results show that, taking into account the random density of the population,

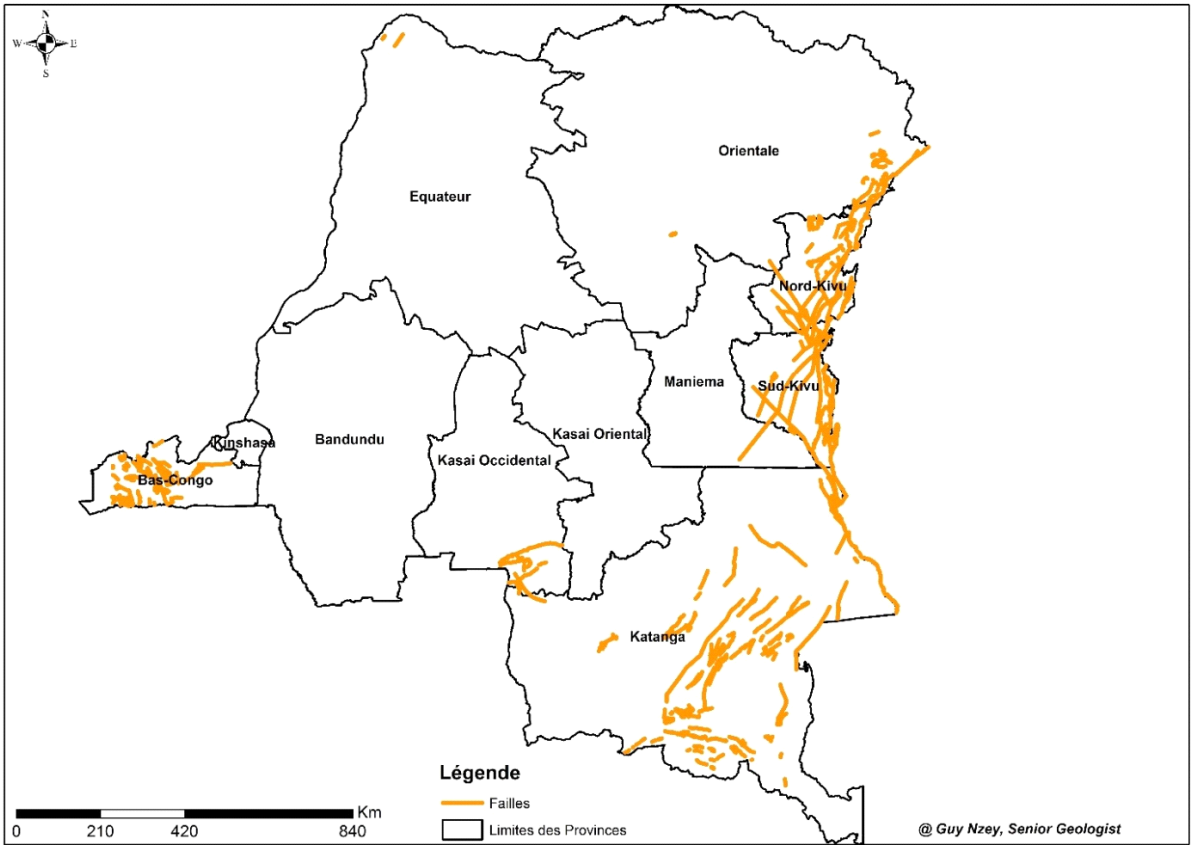

Fig.3.23: structural map of the DRC(C.R.G.M, 2016)

The areas of eastern DRC, particularly North and South Kivu, close to the Congolese Rift, present the highest seismic risk. However, other parameters mentioned above can modify it (Mukange and al., 2015).

3.3.9. COMPARATIVE STUDY DRC, USA, AFRICA AND INDONESIA

In order to deepen our model, it is imperative to extend the research to other areas including the African Continent, Indonesia and the Pacific coast of Central America.

3.3.9.1. Characterization of the seismicity of the African continent

Using the code in table (3.10), the results for the African continent, in particular the seismic level expressed by the modulus, are converted into a map (Fig. 3.24) and into a curve (Appendix III).

Table 3.12. : Color match and Seismic level (N)

Module (Seismic level)	N≤25	25≤N≤42	42<N≤46	60<N<75
Color Code	Blue	Green	Yellow	Purple-Orange-Red

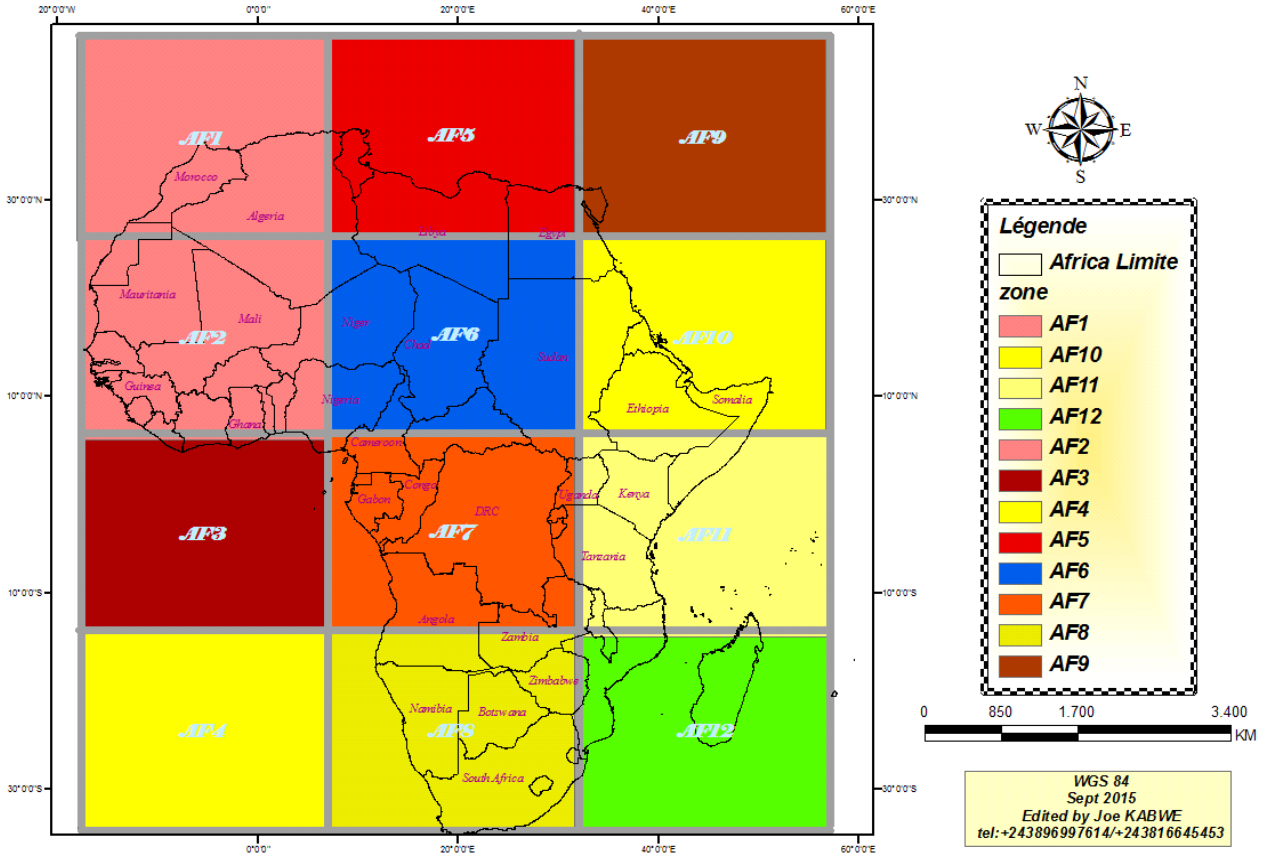

Fig. 3.24: Characterization of the seismic activity of the African continent

This characterization highlights the similarities and differences in the seismicity of various areas of the African continent. These areas are squares of side five degree each.

3.3.9.2. Comparison of seismic structures using the resemblance rate

We are interested in carrying out a comparative study of the structures of the DRC, the Pacific coast of Central America (noted, USA) and Indonesia (Fig.1.3). We do this by using the similarity rate parameter and the color code (Table 3.13 and Fig.3.25). In evaluating the value of the resemblance rate, the Zone-Depth G1 (0-5km) of the DRC is taken as the unit of measurement.

Table 3.13: Legend relating to the similarity rate

Similarity Rate	Color
0%	
] 0-25]	
] 25-50]	
] 50-75]	
] 75-100[	
100	

From Figure (3.25), we draw the following observations:

- The same color is synonymous with structural equality,
- The hypocentres go, in increasing order, from the DRC to Indonesia, via the Pacific coast,
- Although both Indonesia and the Pacific coast are all marked by reverse fault earthquakes, nevertheless the earthquakes of Indonesia (deep earthquakes) are deeper than those of the Pacific Coast (intermediate earthquakes;Zana,2018),
- With a few exceptions, between 30 and 170 km deep, the three structures are identical.

ISSN No:-2456-2165

AREA- DEPTH (km)	STRUCTURE (USA)	STRUCTURE (DRC)	STRUCTURE (INDONESIE)
G1 (0-5)			
G2 (5-10)			
G3 (10-15)			
G4 (15-20)			
B1 (20-25)			
B2 (25-30)			
B3 (30-35)			
B4 (35-40)			
SM1 (40-105)			
SM2 (105-170)			
SM3 (170-235)		SEISMIC INACTIVITY	
SM4 (235-300)		SEISMIC INACTIVITY	
SM5 (300-400)	SEISMIC INACTIVITY	SEISMIC INACTIVITY	
SM6 (400-500)	SEISMIC INACTIVITY	SEISMIC INACTIVITY	
SM7 (500-650)	SEISMIC INACTIVITY	SEISMIC INACTIVITY	

Fig. 3.25. : Dynamics of the internal structures of three zones as a function of the rate of resemblance

3.3.9.3. Comparison of seismic structures using signatures or fingerprints

As before, we transform the results expressed in modulus or seismic level for each Cell, into curves, called signatures and footprints (appendix I, II, III,IV).

Comparison of these signatures (Fig. 3.26) observes the following:

- All these signatures (Fig.3.23a-d) have a central symmetry,
- The signature of the AFRI 10 zone, located in the Afar triangle in the Red Sea and the Gulf of Aden (Fig. 3.21), is antisymmetrical or reversed compared to the other three, which, they are identical or almost,
- The AFRI 10 signature highlights the fact that the seismic activity is less intense at the center ("V" shape of the signature, at the central axis) than on either side of the central axis. or the seismic level is almost constant (parallel lines).

Figure (3.26a) therefore perfectly accounts for the structure of the seismicity in the Afar triangle; indeed, the left wing of this figure represents the Red Sea, while the right wing reproduces the Gulf of Aden. So we can say that our model is reasonable.

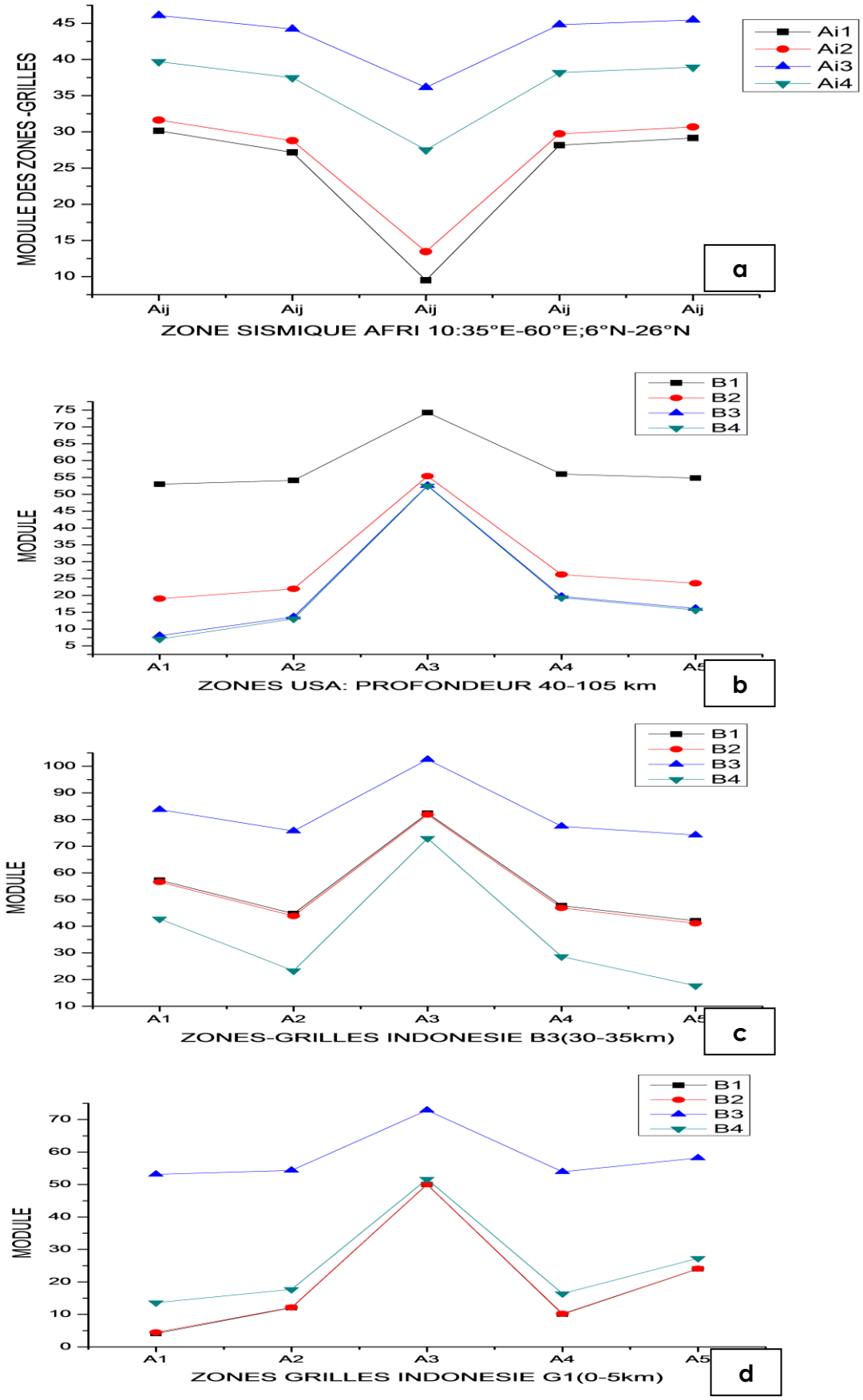

Fig. 3.26: Some remarkable structures mapped in various places: signatures

ISSN No:-2456-2165

Our characterization model makes it possible to "map" various parts of the globe and to compare them: knowing the characteristics and the structure of the zone A, if the unknown zone B presents, after calculation, the same structure or value of the parameters as A, then B has the same characteristics as A. This is how this model can be used to prospect for unknown geological structures.

Below we present two similar structures from the DRC and Indonesia.

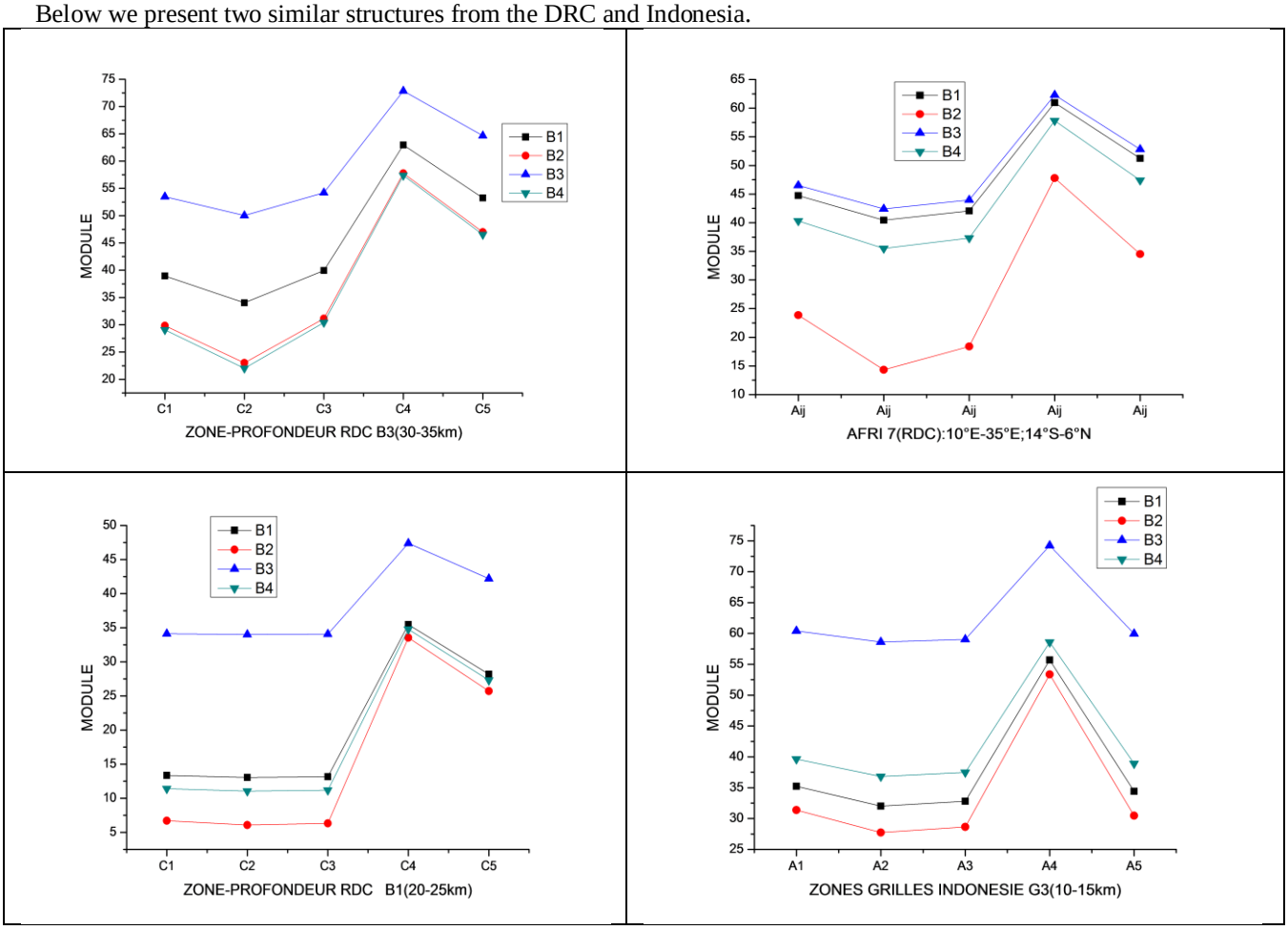

Fig. 3.27: Comparison between some structures in the DRC zone and those in Indonesia

The structure of Indonesia G3, between 10 and 15 km, is almost identical to that of the DRC, better with the DRC at B1 (20-25km); oddly enough, these two areas are full of copper and oil in some places. In addition, we can establish the following relationships between the seismicity of these two zones:

$$\boldsymbol{Y_{L4(G3\ INDO)} = Y_{L4(RDC)}} \quad \textbf{(3.14)}$$

$$\boldsymbol{Y_{L3(G3\ INDO)} = Y_{L3(RDC)} + 13,0} \quad \textbf{(3.15)}$$

These relationships can be reassessed later to reflect their dynamics.

Furthermore, there is a resemblance between the following two structures, one from the DRC (SM1), the other from Indonesia (SM2).

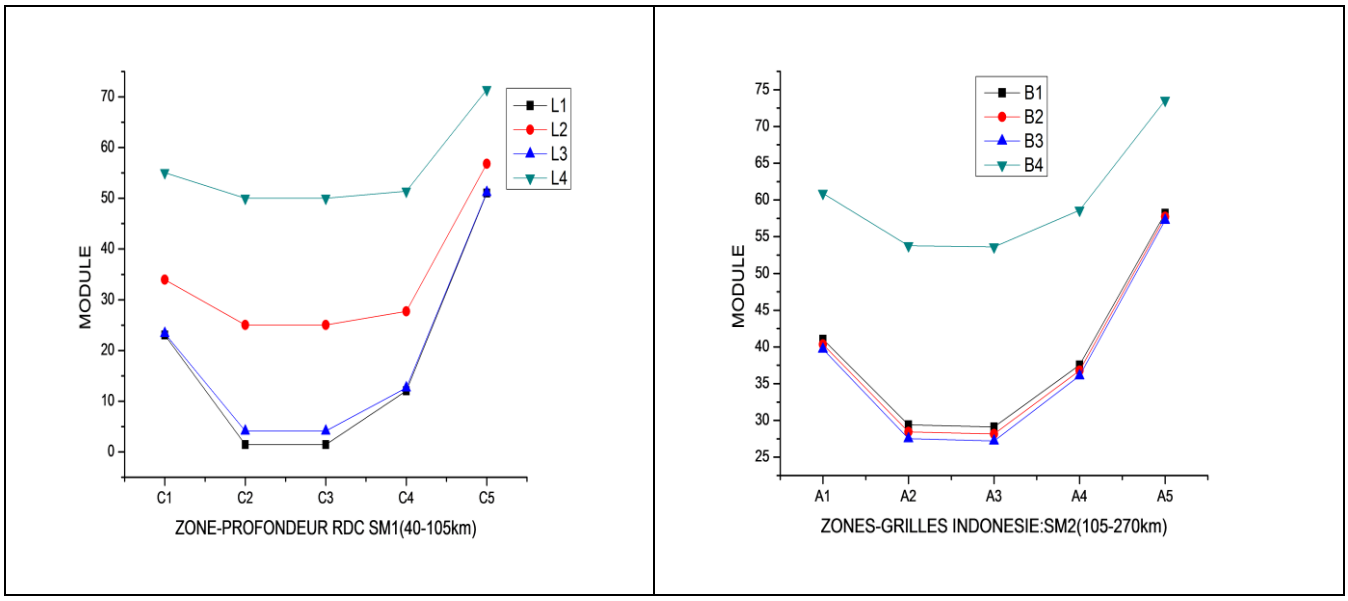

Fig. 3.28: Comparison between the structure SM1 of the DRC and SM2 of Indonesia

VI. GENERAL CONCLUSION

The application of the unified characterization scale to the characterization of the seismicity of the Democratic Republic of Congo (DRC: 10°E-35°E; 14°S-6°N) and its extension to the African Continent zones (15°W-60°E: 25°S-55°N) -, Indonesia (125°E-150°E;10°S-10°N) and the Pacific coast of Central America (115°W-90°W; 0°N-20°N) for the period from 1975 to 2013 provided satisfactory results. Indeed, the identification of the seismic species in each Zone-Grid (mesh) and the attribution of the seismic level (modulus) and the corresponding color code, the use of the similarity rate parameter as well as the introduction of the representation of an area as a vector, allowed allowed :

- **The development of a device (clock) called Acti-seismometer** to better follow the seismic activity and the geodynamics of an area
- **The characterization of the seismicity using curves**

Observation of these curves, synonymous with signature or imprint, indicates the following:

- The DRC's seismicity is diversified both from West to East and from North to South, but it is however very intense towards the Rift zones (in the East of the country),
- These curves show a clear distinction between the Rift zones with high seismicity and those outside the Rift with weak seismicity; the limit between these two zones is located at 25 ° E.

- **The characterization of the internal structure or seismic profile (tomography)**

Observation of the average curve describing the seismic activity as a function of depth indicates that the structure is subdivided into two:

- The granite layer (G1-G4): it is characterized by a line of decreasing slope modeled by figure (3.10) on the left,
- The basaltic zone (B1-B4) to the sub-mantle zone (SM1): the structure is characterized by a parabola of concavity turned downwards whose axis of symmetry is located at B4 (on the abscissa) with a seismic level maximum of 67 (on the y-axis),

- **The calculation of the Ratio and Gradient parameters of the seismic level of the structure**

The results of the "ratio" calculation indicate:

- An overall ratio greater than unity (1), meaning that the seismic activity increases with depth,
- A very high Ratio at SM1 (40-107km) for zones A42 (Zone Kivu) and A44 (Rift Zone of Upemba / Haut-Katanga). Structurally speaking, in these places, the faults are complex for these areas (Fig. 3.22-23),
- An almost identical behavior for zones A43 (Tanganyika zone) and A41 (South Sudan zone), because we observe that their curves are almost identical, synonymous with a structural identity.

The results of the calculation of the "gradient" of the seismic level indicate, on the one hand, a structure subdivided into three parts, all wavy in shape:

- **The granite part (G1-G4):** here, the amplitude of the seismic levels of the curves varies in the interval [-20, + 20]; therefore a positive difference from the peaks of +40,
- **Most basaltic (G4-B3),** the amplitude of the seismic levels of the curves varies in the interval [-20, +50]; therefore a positive difference from the peaks of +70,
- **Most of the sub-basaltic layer (B3-SM2),** the amplitude of the seismic levels of the curves varies in the interval [10, -60]; therefore a negative difference from the peaks of -70. This translates to a stability of the structure seismically speaking.
- In short, the result of these observations can be described by the curve in red represented by the Kivu zone (A42): it is on average a Gaussian whose peak is 50 and is located at B2 (25-30 km). its band width is 5km. Indeed, figure (3.20) indicates the presence of crossed faults, that is to say, both of NE-SW and NW-SE orientation.

- **Characterization using zoning maps: seismic tomography**

From this aspect, it emerges that:

- The seismicity marks a clear difference between the zones of the rift (25-35 ° E), of strong activity and those outside the rift (10-25 ° E), of weak activity; however, the C3 zone (20-25 ° E), especially in the Upemba rift in South Katanga (A33) constitutes a suture zone (transition) between the two,
- Zones A22, A21 and A12 are seismically stable (low level) and located in the sedimentary zone (Congolese craton) where geophysical research has revealed the presence of hydrocarbons (Biliki et al., 2021),
- From the previous observation follows the conclusion that the seismicity of the rift migrates and the hypocenters increase overall from North to South.

- **Comparison of areas through the rate of resemblance**

This comparison highlights three facts:

- This is the difference between the seismicity of the west of the DRC and that of the east. In this case, we observe that the hypocenters become more and more superficial as they go from the zones.
- Presence of La Depondeur G1 (0 - 5 km) corresponds to a sedimentary layer at A22 and A32 at a depth of 0-5km where gravity and geomagnetic prospecting revealed the presence of hydrocarbons (Biliki et al., 2021).
- The possibility of monitoring the dynamics of the structure: for this purpose, a study was carried out on the Pacific coast area of Central America for the period from 1978 to 2013.

- **Seismic risk assessment**

By calculating the seismic hazard and the vulnerability factor using our model, the seismic risk calculated in each Grid Zone of the DRC indicates that the following areas present the highest risk:

- Zone A23 (Kinshasa-Bandundu and surroundings), following the presence of the Kinshasa nuclear power plant, the Atlantic Ocean and less than 500km (in Gabon) where minor earthquakes are recorded and the presence of faults observed in its surroundings, not to mention the high density of the population.
- Zone A42 (Kivu): here, this factor is important following the presence of volcanoes (Nyiragongo, Nyamulagira, etc.) whose flow is heading towards the city, presence of Lake Kivu containing harmful gas (methane gas and carbon dioxide) and the presence of complex faults observed therein as well as the high population density.

- **The comparative study of the DRC, Pacific Coast of Central America, Africa and Indonesia areas**

In order to deepen our model, it was imperative to extend the research to other areas, including the African Continent (15 ° W-60 ° E: 25 ° S-55 ° N) -, Indonesia (125 ° E-150 ° E; 10 ° S-10 ° N) and the Pacific coast of Central America (115 ° W-90 ° W; 0 ° N-20 ° N) for the period from 1975 to 2013 .

The following aspects were discussed:

- **The characterization of the seismicity of the African continent**

This continent has been subdivided into twelve square areas of side five degrees. This characterization highlights a similarity and difference in seismicity between the twelve zones.

- ✓ The signature in the area of the Afar triangle (55 ° E-60 ° E; 45 ° N-50 ° N) perfectly reflects its symmetrical seismic structure; indeed, the left wing of this figure represents the Red Sea, while the right wing reproduces the Gulf of Aden. So we can say that our model is reasonable.

- **Comparison of seismic structures**

From this comparison, we draw the following observations :

- ✓ The hypocenters go, in ascending order: DRC - Pacific coast - Indonesia,
- ✓ With a few exceptions, between 30 and 170 km deep, the three structures are identical.
- ✓ A strong resemblance of signatures, synonymous with structural identity, existence of symmetries of signatures,
- ✓ The signatures reveal the structure of the subsoil (Afar triangle, Red Sea, Gulf of Aden)
- ✓ The structure of Indonesia G3, between 10 and 15 km, is almost identical to that of the DRC, better with the DRC at B1 (20-25km); oddly enough, these two areas are full of copper and oil in some places. In addition, we can establish the following relationships between the seismicity of these two zones.

Our characterization model will make it possible to "map" various parts of the globe and compare them with one another with the possibility of exploiting it for geological prospecting: For a better assessment of the seismic risk, the surface area of the study area should be reduced, which will protect our model from overestimating the seismic hazard.

REFERENCES

[1]. Bantidi M., Wafula M., Mavambou, Mukange B., Zana Nd., (2014a). Probabilistic assessment of seismic hazard in Lake Tanganyika Rift accounting for local geologies conditions. 2015. *International Journal of Geology, Agriculture and Environmental Sciences*. Vol.03 Issue 02 (April 2015), pp24-29.

[2]. Bantidi M., Mukange B., et Zana N., (2014b). Structure de la sismicité de la Branche occidentale des Rifts Valleys du système des Rifts Est-africains ; de 1954 à 2010, *International Journal of Innovation and Applied Studies*, ISSN 2028-9324 Vol. 9 No. 4 Dec. 2014, pp.1562-1581.

[3]. Biliki K;. et al.,(2021). Interpretation of Gravity Data and Contribution to the Study of the Geological Structure of the Province of Mai-Ndombe in DR. Congo: Implications in the Exploration of Hydrocarbons. International Journal of Innovative Science and Research Technology, Volume 6, Issue

4, April – 2021, pp213-921.

[4]. Borden J-P., (1988). *Biologie-Géologie*. Première S. Paris: Bordas

[5]. Lay T., et Wallace T., (1995). *Modern Global seismology*. New-York : Academic Press

[6]. Mavonga Tuluka G., (2009).*Seismic hazard assessment and volcanogenic seismicity for the Democratic Republic of Congo and surrounding areas, western Rift valley of Africa*. Thèse de Doctorat : University of the Witwatersrand (Johannesburg), Faculty of Sciences.

[7]. Mukange B., Bantidi M., Zana Nd., (2013). Structure de la sismicité de la Branche orientale des Rifts Valleys du système des Rifts Est-africains ; de 1954 à 2010. *Revue Congolaise des Sciences Nucléaires.* vol.27, pp 151-169.

[8]. Mukange B., Bantidi M., Zana L., Wafula M., Zana Nd., (2015). The isoseismal map and their implication to underlining ground degree of heterogeneity (Kabalo quake's case, September 11, 1992, magnitude 6.7, Upemba Rift). *Greener Journal of Geology and Earth Sciences*, vol. 3 (2), pp 030-042

[9]. Mukange B., (2016). *Conception d'un modèle physique pour la caractérisation et la surveillance de l'activité sismique et son implication géologique (Cas de la République Démocratique du Congo).* Thèse de Doctorat : Université de Kinshasa, Faculté des Sciences. Département de Physique.

[10]. Mukange Besa, (2021). *Cours de Géophysique générale*. Université de Kinshasa, Faculté des Sciences.

[11]. Mukange B.,(2021a). **Design of a unified scale for the characterization of seismic activity.** International Journal of Innovative Science and Research Technology, in press.

[12]. Muswema Lunguya, (2015).*Etude par modélisation de la dispersion atmosphérique des radioéléments générés par le réacteur nucléaire Triga mark II de Kinshasa lors d'un accident hypothétique*. Thèse de Doctorat : Université de Kinshasa, Faculté des Sciences, Département de Chimie.

[13]. Ngindu D. et al., (2021). New Faults from the Geodynamics of South Katanga in D.R.Congo. International Journal of Innovative Science and Research Technology, Vol (6) Issue 1(January 2021),pp1596-1689.

[14]. Tondozi K. et al, (2018). Interpretation of gravity anomalies maps and contribution to the structural study of a sedimentary basin of major petroleum interest: Case of the Busira sub-basin in the Central basin of the DR Congo, IJIAS Vol. 24 N°1, p. 68-88.

[15]. Wafula M., D. Atiamutu et M. Ciraba, (1999). Activité séismique dans les Virunga (Rép.Dém. Congo) liée aux éruptions du Nyiragongo et Nyamuragira, deNovembre 1994 à Décembre 1996. *Mus. roy. Afr. centr. Tervuren Belg., Dépt.Géol. Min. Rapp. Ann. 1997 & 1998*, pp. 309 - 319.

[16]. Wafula M.D., Kasereka M., Rusangiza K., Kuvuke K., Mukambilwa K., Ciraba M. &Bagalwa M., (2009). The Nyamulagira Volcanic Eruption on November 27, 2006,Virunga Region, D.R. Congo. *Cahiers du CERUKI, Numéro Spécial CRSN-Lwiro(2009)*, pp. 108 - 115.

[17]. Wafula M.D, Zana A. Kasereka M. and Hamaguchi H., (2011a). The Nyiragongo volcano: A case study for the Mitigation of Hazards on an African Rift Volcano, Virungaregion, Western African Rift Valley, 32 pp.
Disponible sur: *http://iugg georisk.org/presentations*

[18]. Wafula M., (2011b). *Etude Géophysique de l'Activité Volcano-Séismique de la Région des Virunga, Branche Occidentale du Système des Rifts Est-Africains et son Implication dans la Prédiction des Eruptions Volcaniques.* Thèse de Doctorat : Université de Kinshasa, Faculté des Sciences.

[19]. Zana N, (1977). The Seismicity of the Western Rift Valley of Africa and related problems, *Doctorat Theses*, Tôhoku University. 189 pp.

[20]. Zana N. and K. Tanaka, (1981). Focal mechanism of major earthquakes in the WesternRift Valley of Africa, *Tôhoku Geophys. Journ. (Sci. Rep. Tôhoku Univ. Ser. 5)*, Vol.28, Nos 3-4, pp: 119 - 129.

[21]. Zana Ndontoni A., (2004), Cours de Géophysique : Introduction à la géophysique générale, UNIKIN, Kinshasa

[22]. Zana A., (2010), Détonateur Potentiel de Tsunami au lac Kivu, Conférence débat, OVG, Goma.

ISSN No:-2456-2165

Appendix I: signatures (impressions) of internal structures of the DRC (10°E-35°E; 14°S-6°N) depending on the depth

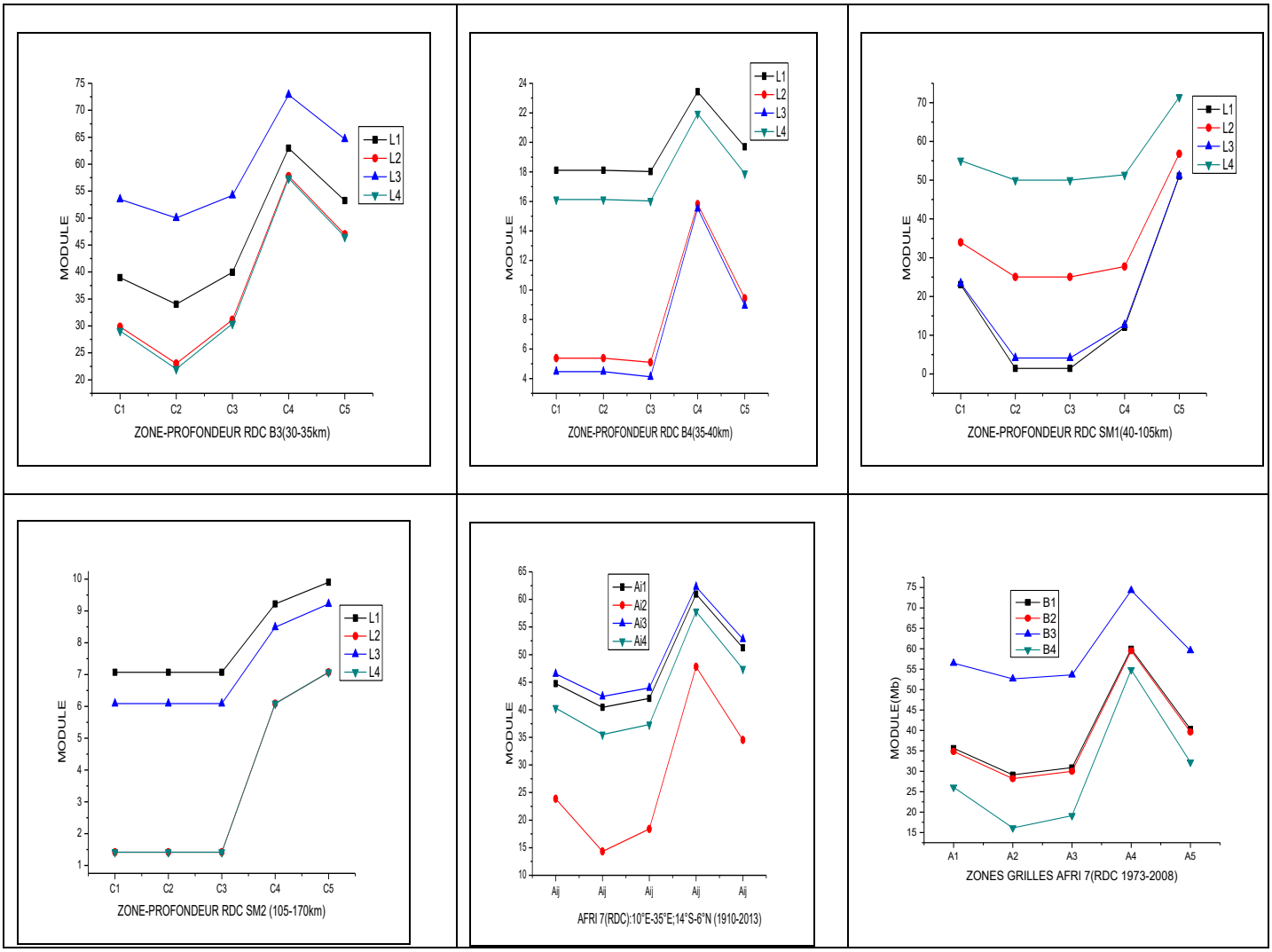

Appendix I (continued): signatures (impressions) of internal structures of the DRC (10°E-35°E; 14°S-6°N) depending on the depth

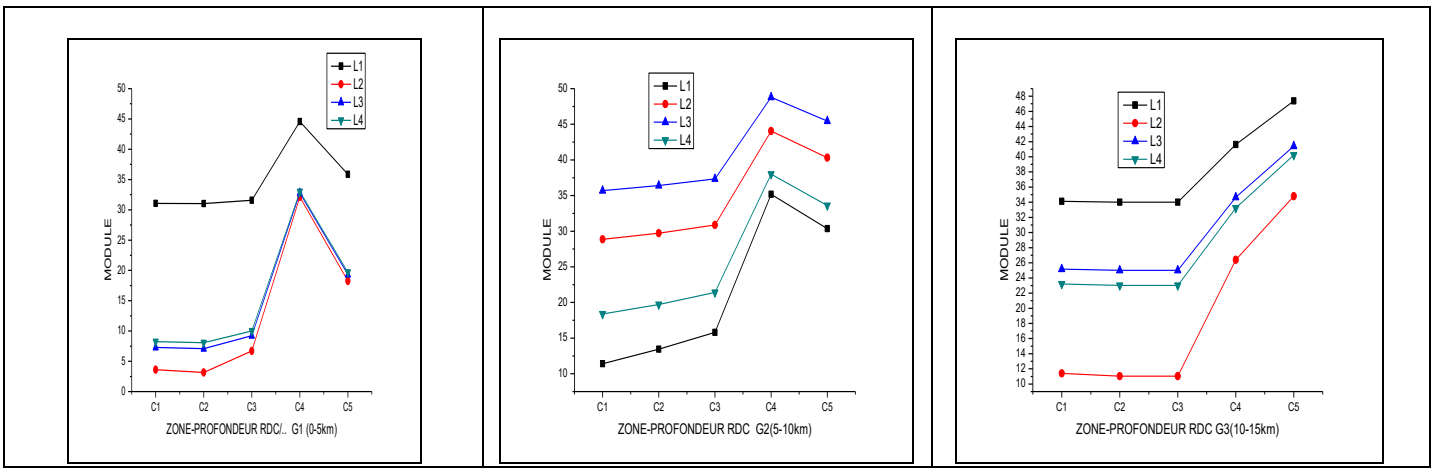

ISSN No:-2456-2165

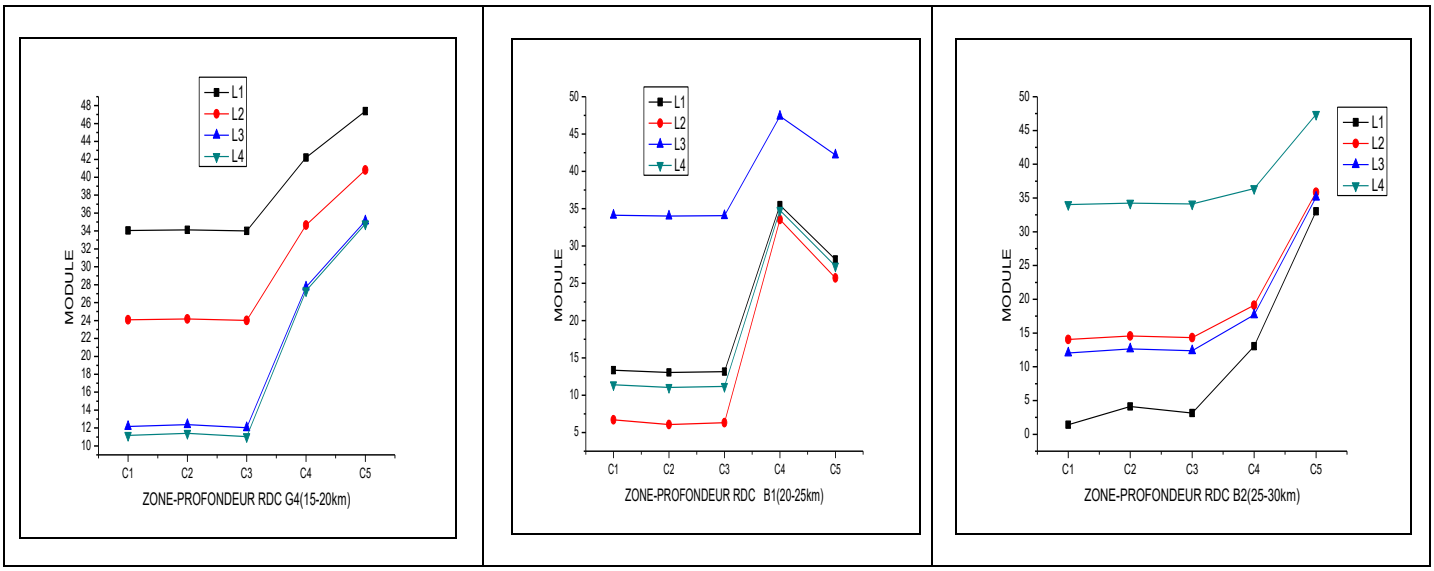

APPENDIX II: signatures (impressions) of the internal structures of the African continent (15°W-60°E; 25°S-55°N) depending on the depth

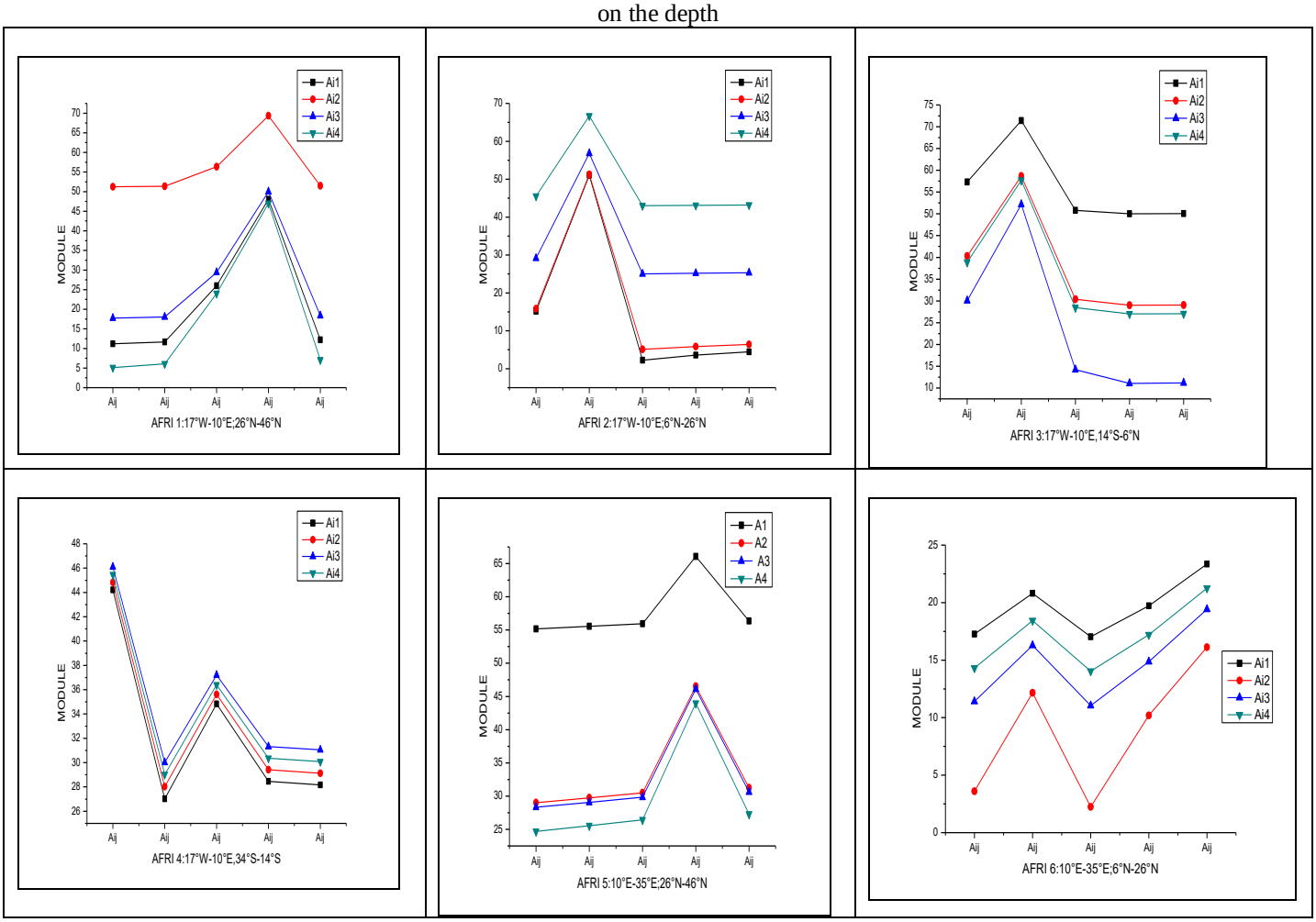

APPENDIX II (CONTINUED): signatures (impressions) of the internal structures of the African continent (15°W-60°E; 25°S-55°N) depending on the depth

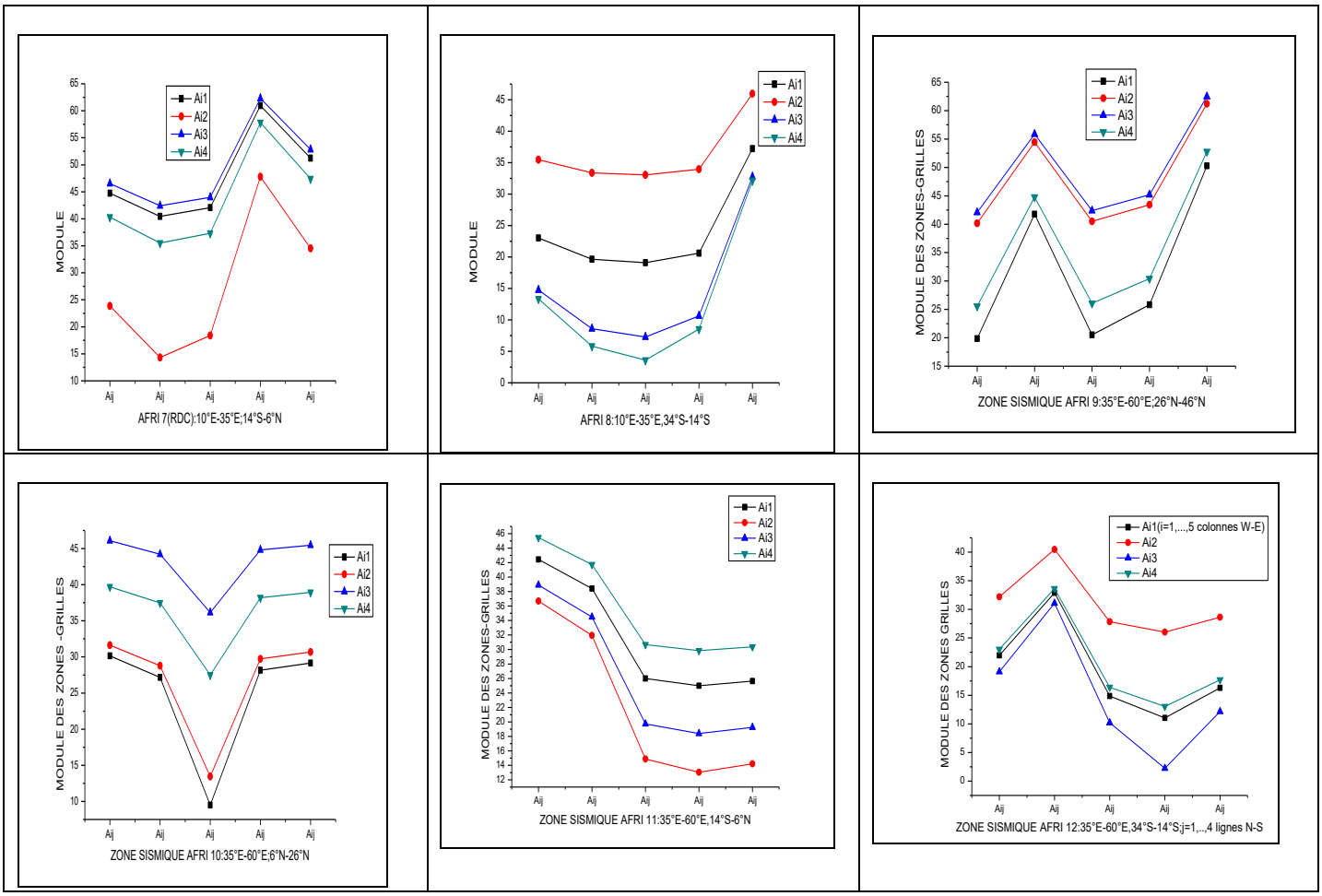

APPENDIX III: signatures (impressions) of Indonesia's internal structures (125°E-150°E; 10°S-10°N) depending on depth

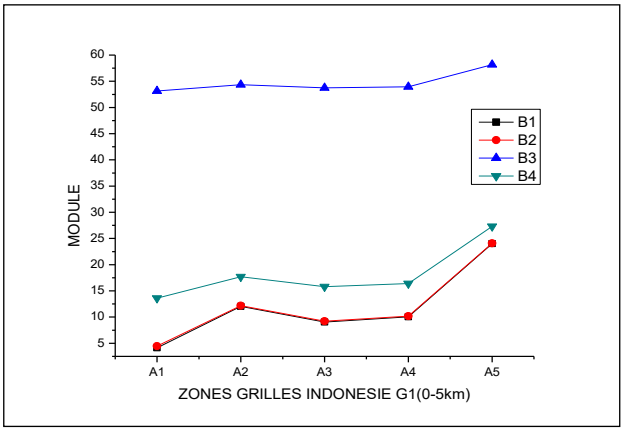

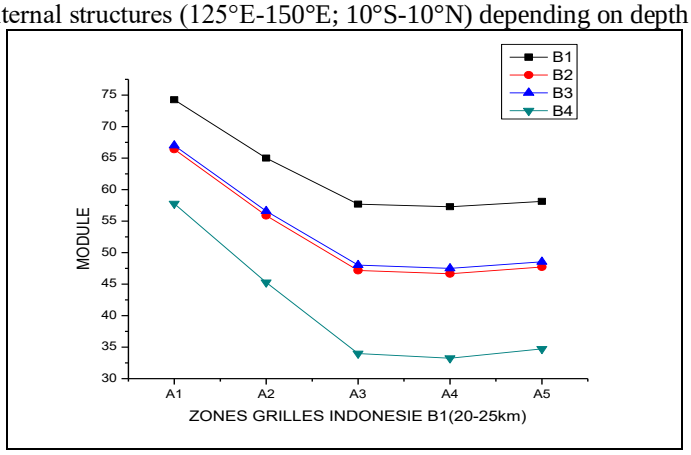

ISSN No:-2456-2165

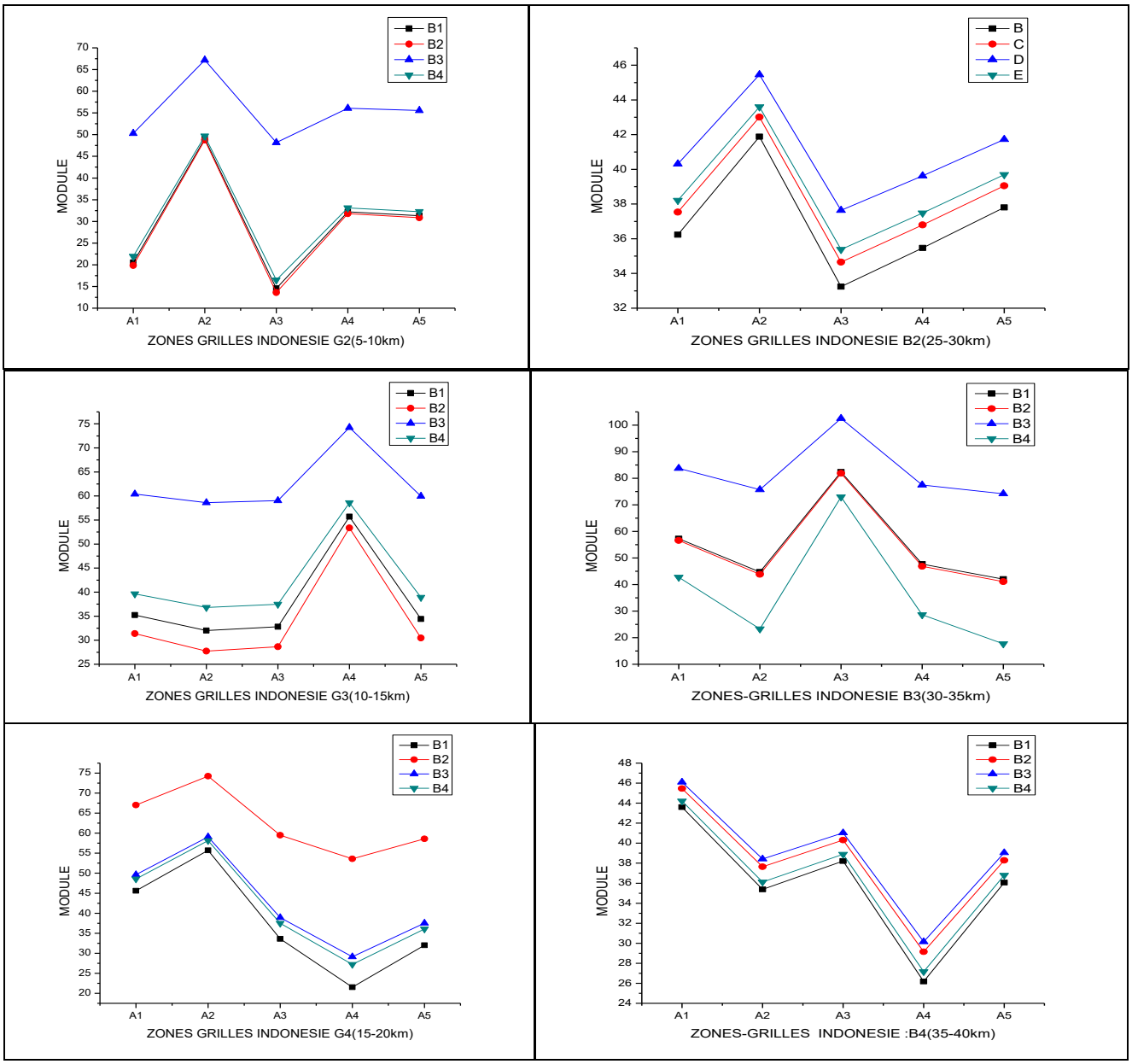

APPENDIX III (CONTINUED): signatures (impressions) of Indonesia's internal structures (125°E-150°E; 10°S-10°N) depending on depth

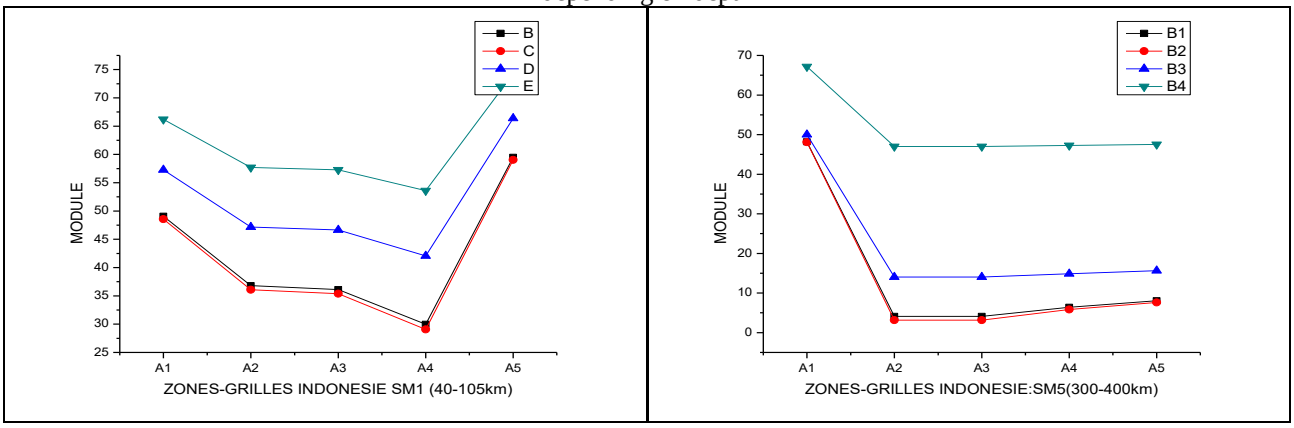

ISSN No:-2456-2165

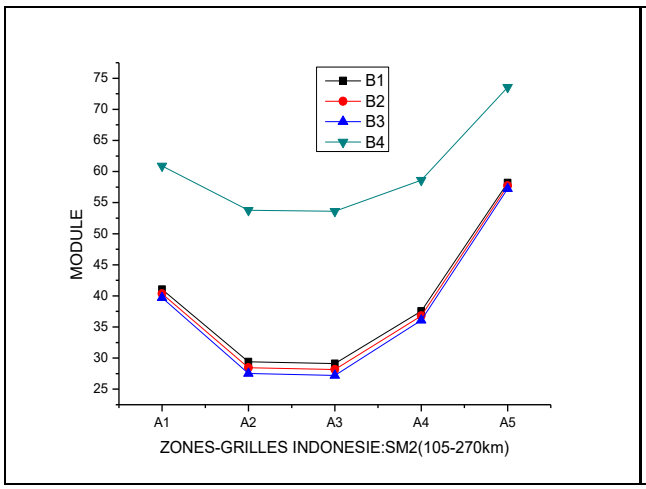

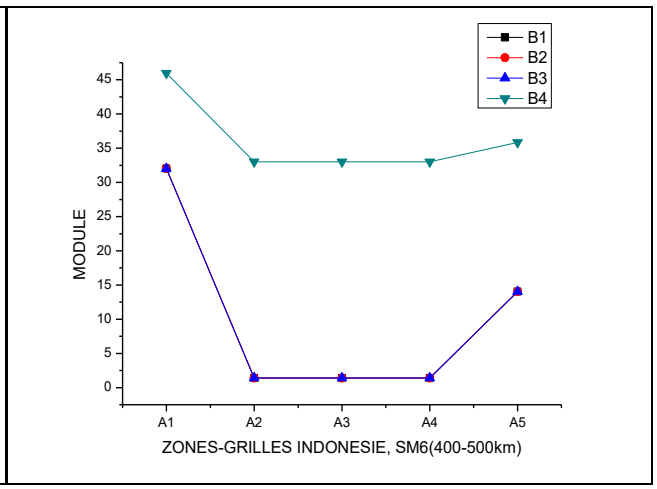

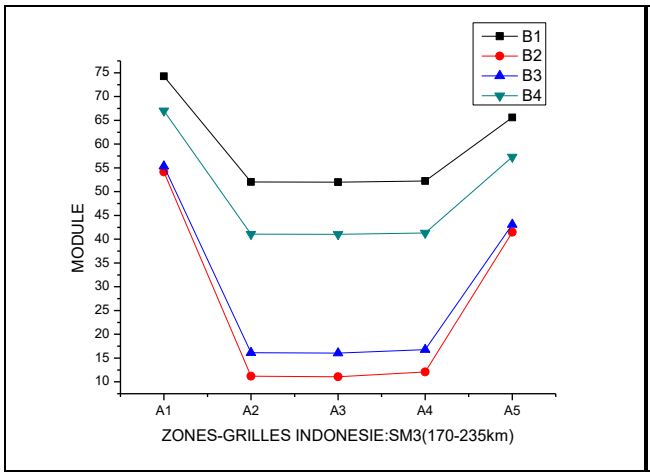

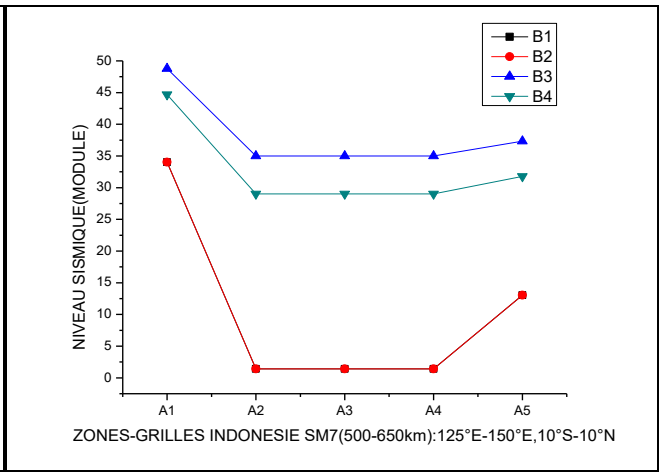

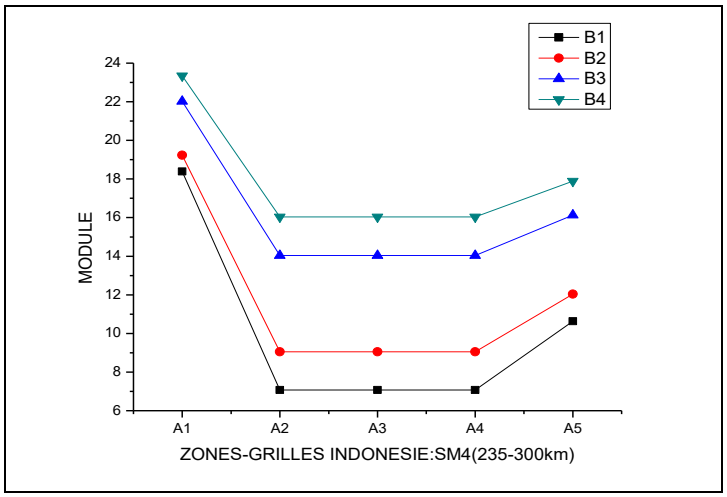

ISSN No:-2456-2165

ANNEX IV: signatures or impressions of internal structures of the pacific coast of central America (115°W-90°W; 0°N-20°N) depending on depth

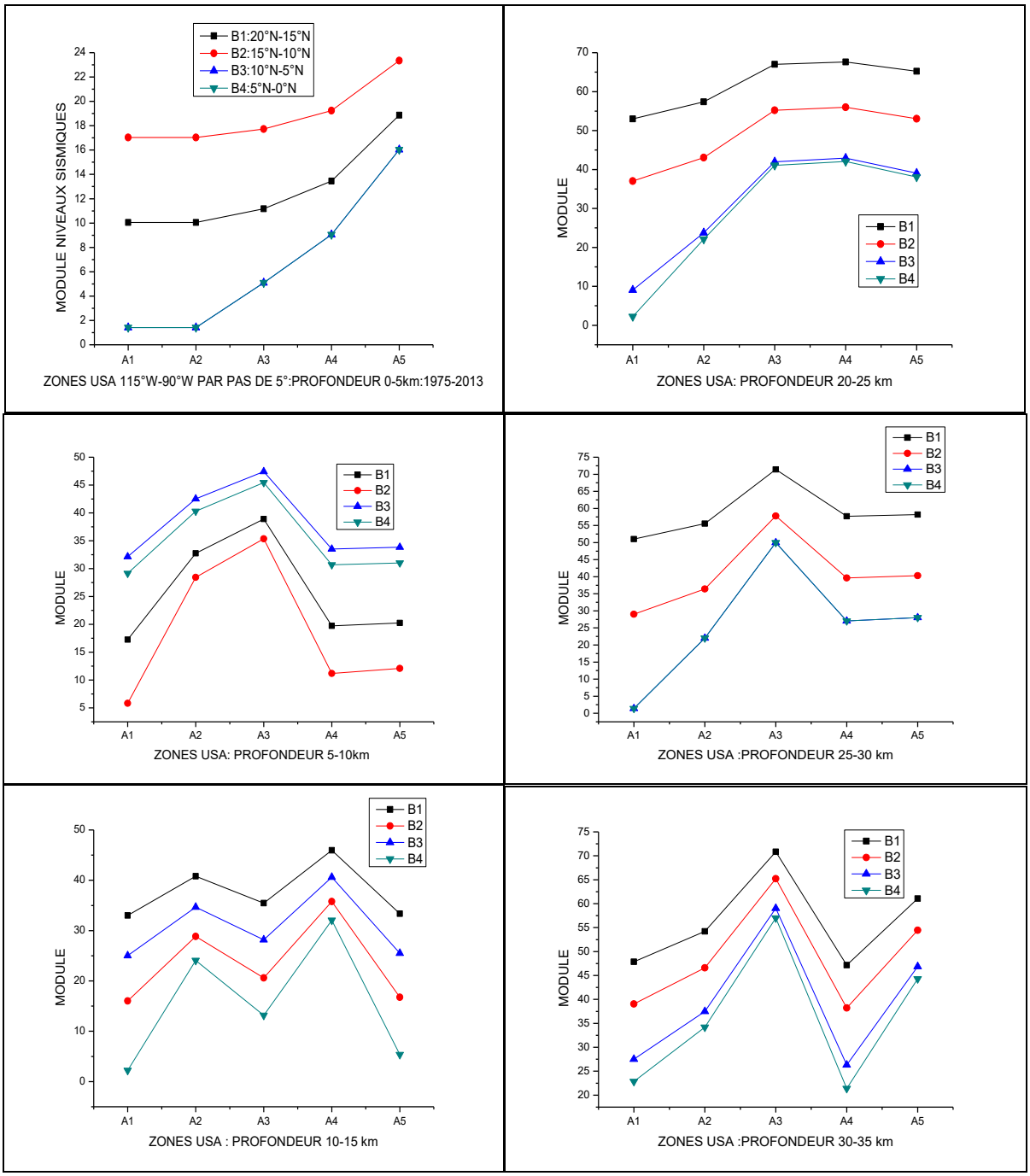

ISSN No:-2456-2165

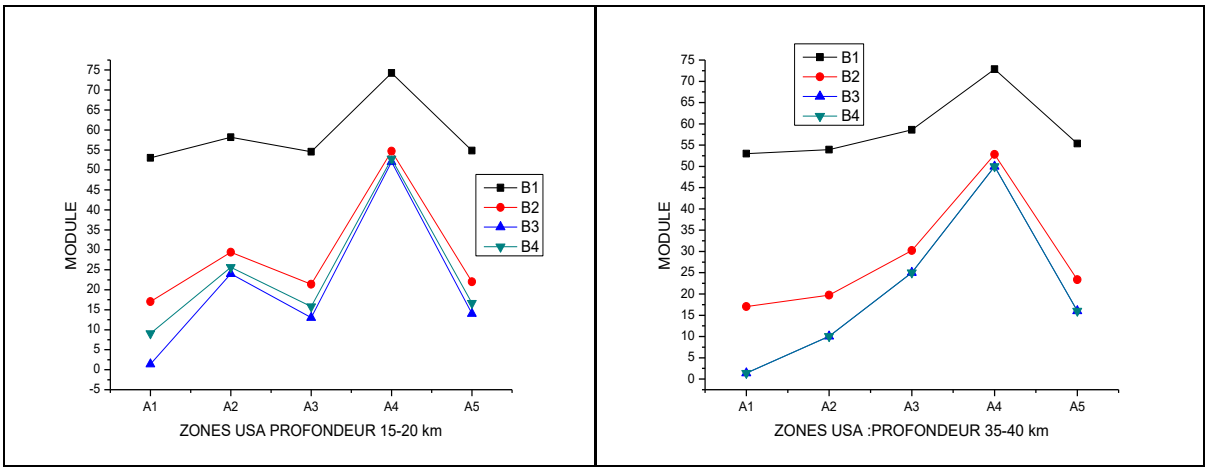

ANNEX IV (CONTINUED): signatures or impressions of internal structures of the pacific coast of Central America (115°W-90°W; 0°N-20°N) depending on depth

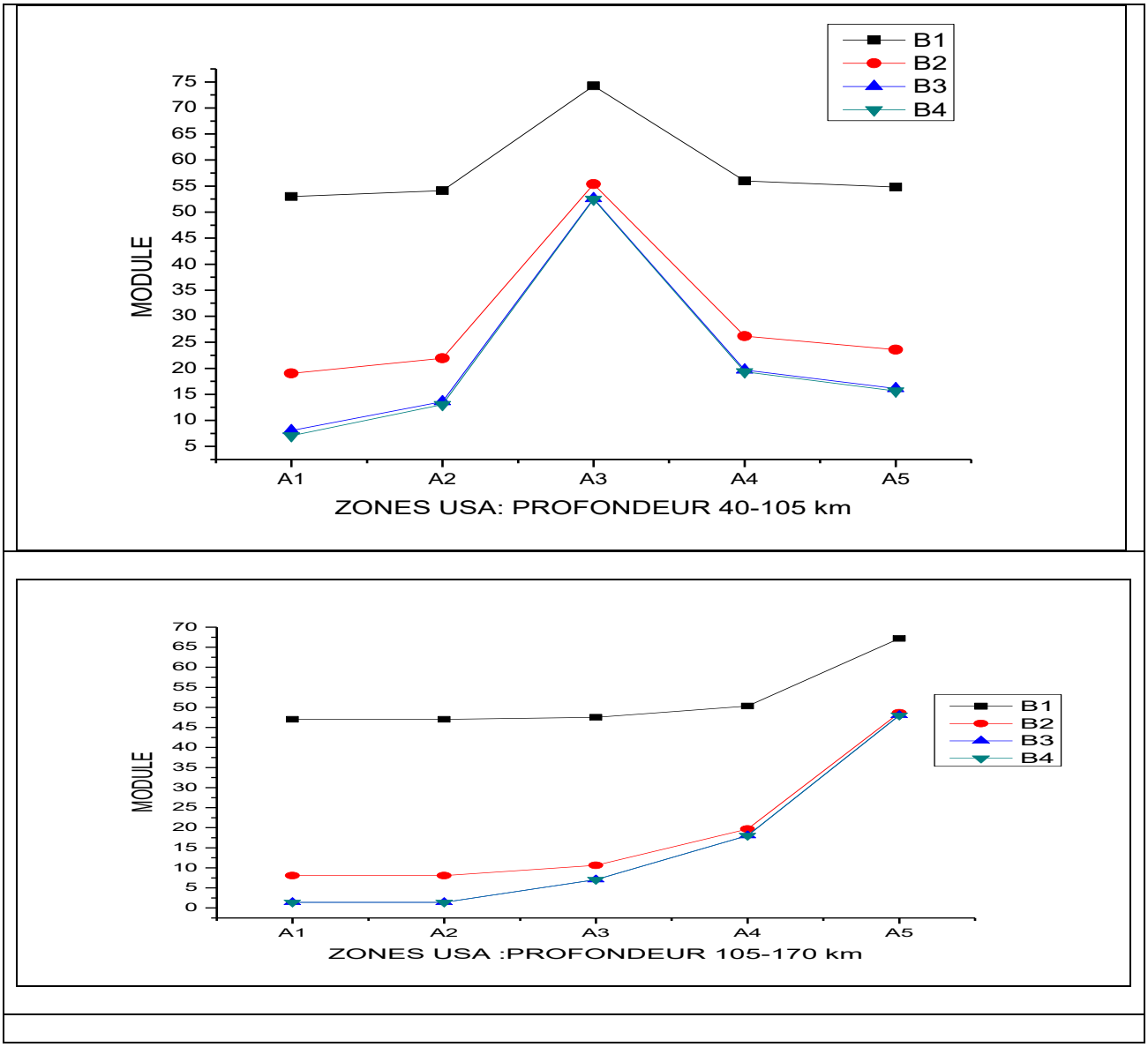

ISSN No:-2456-2165